INL/INT-10-17854

RERTR-10A Test: Overview and Breach Assessment

Daniel M. Wachs, Ann Marie Phillips,
Eric L. Shaber, Barry H. Rabin,
Curtis R. Clark, Adam B. Robinson

February 2010

DISCLAIMER

This information was prepared as an account of work sponsored by an agency of the U.S. Government. Neither the U.S. Government nor any agency thereof, nor any of their employees, makes any warranty, expressed or implied, or assumes any legal liability or responsibility for the accuracy, completeness, or usefulness, of any information, apparatus, product, or process disclosed, or represents that its use would not infringe privately owned rights. References herein to any specific commercial product, process, or service by trade name, trade mark, manufacturer, or otherwise, does not necessarily constitute or imply its endorsement, recommendation, or favoring by the U.S. Government or any agency thereof. The views and opinions of authors expressed herein do not necessarily state or reflect those of the U.S. Government or any agency thereof.

INL/INT-10-17854

RERTR-10A Test: Overview and Breach Assessment

Daniel M. Wachs, Ann Marie Phillips, Eric L. Shaber, Barry H. Rabin,
Curtis R. Clark, Adam B. Robinson

February 2010

Idaho National Laboratory
Idaho Falls, Idaho 83415

EXECUTIVE SUMMARY

The Reduced Enrichment for Research and Test Reactors (RERTR) program has been working to develop a very high density nuclear fuel for research and test reactors based on uranium-molybdenum alloys for the last decade. Over the course of that development, the program has conducted 15 irradiation campaigns, testing a total of 321 fuel plates in the Advanced Test Reactor (ATR), in addition to collaborating with several foreign irradiation programs. These studies have shown that to a high burnup uranium-molybdenum alloy monolithic fuel is stable, exhibiting only modest swelling. As the next step, monolithic fuel performance research is currently focused on optimization of the fuel/clad interface. This interface may deteriorate throughout irradiation due to the formation of undesirable U-Mo/Al reaction products.

The RERTR-10 mini-plate test was conducted to evaluate the performance of several different modifications to this interfacial layer under irradiation. The primary objective of the RERTR-10A was to compare the effectiveness of a zirconium diffusion barrier to a silicon-modified fuel/clad interface. To observe performance behaviors that differentiate these fuel designs, the fuel plates must be irradiated to high burnup (> ~100% LEU equivalent) and the fuel/clad interface must be subjected to tensile forces during irradiation. To achieve this, the RERTR-10 mini-plate test was oriented perpendicular to the neutron flux gradient so that the inner edge of the plate experiences larger fission densities (and thus swelling) than the outer edge. A tensile load at the fuel/clad interface is created by the differential swelling between the two edges. The RERTR-10 campaign was sub-divided into the RERTR-10A and RERTR-10B, which were fabricated with the Hot Isostatic Press (HIP) process and friction bonding (FB) fabrication processes, respectively.

During irradiation, a cladding breach was identified on the RERTR-10A test during ATR Cycle 143. Failure analysis, including in-canal inspection, non-destructive examination, and destructive examination, showed that a small blister had formed and ruptured, releasing a small amount of fission products. The root cause of the breach was the formation of a thick oxide layer, which increased the surface temperature on one side of the mini-plate, leading to formation of the blister on the fuel plate surface.

Protection of the ATR cladding material from excessive oxidation during irradiation is currently provided by a fully aged continuous boehmite layer that is created through autoclaving prior to irradiation. When fully aged, boehmite is a thermally stable crystalline surface film under irradiation. Further investigation of the RERTR-10A mini-plate concluded that it is possible that an improperly aged boehmite layer contributed to formation of the oxide layer. The autoclaving process used on the RERTR plates has now been modified to match the current ATR process to ensure proper boehmite ageing, which will provide better oxidation protection in the future.

In addition, a detailed review of the RERTR-10A fabrication process was conducted, concluding that the fabrication process and process controls are being conducted properly. Several good practices that were being performed were added to the process documentation, to ensure their continuation in the future.

Post-irradiation examination (PIE) of the RERTR-10A mini-plates showed that the silicon-modified plates exhibited significantly greater swelling, delamination, and fuel-foil cracking than the zirconium barrier plates. It is important to highlight that the breached fuel plate in the RERTR-10A test was a silicon-modified fuel plate. The RERTR-10A test clearly showed the excellent performance of the zirconium diffusion barrier based design and the marginal performance of the silicon-modified design at very severe conditions. As a result, the silicon design will be dropped and the future testing will focus on the zirconium design.

The fuel plate sensitivity may have been enhanced by the presence of fuel/clad delamination near the defect, which could cause an increase in surface temperature that could impact surface oxidation rates. Delaminations can occur either before irradiation (as-fabricated) or during irradiation (irradiation induced). As the fuel behavior under irradiation has been proven to be stable, an assessment was performed to evaluate if pre-existing defects may have gone unidentified during the pre-irradiation fuel plate scanning. This review included examination of the blister anneal test traditionally applied to identify as-fabricated debonds in dispersion fuels to determine if it is appropriate for use on monolithic fuels. In the area that blistered, no debonds were observed, leading to the conclusion that debonds were not a contributing factor in this blister.

It is unlikely that conducting a blister anneal test would have prevented the RERTR-10A failure. First, no debonds were identified that correlated to the blister location, making it unlikely that debonds contributed to the oxide growth and blister formation. Second, studies conducted show that the UT scan is conservative, and the blister anneal test does not reveal debonds that were not indicated with the UT scan. Consequently, it can be concluded that applying the blister anneal test to RERTR-10A would not have prevented the failure as the plate would have passed the blister anneal test.

A generic study of delamination identification in monolithic fuel using the blister anneal and UT scanning process was conducted, as well as a comparison of both techniques during examination of the RERTR-12 mini-plates. These studies showed that during the blister anneal test, blisters formed only in locations where there were existing indications that were identifiable in the UT scan of the as-HIPed plates. Blister annealing results in severe warping and dimensional instability in fuel plates that significantly complicates subsequent fabrication steps. In addition, blister annealing may introduce degradation into otherwise acceptable fuel plates, while not detecting the presence of certain resulting defects so introduced. The studies showed that the UT scan process is more conservative than the blister anneal. The UT scan process should be used as the reference process to characterize bonding in monolithic fuel plates and should be applied formally in the fuel specifications.

CONTENTS

EXECUTIVE SUMMARY iii

ACRONYMS ix

1. DESCRIPTION OF THE RERTR-10A TEST 1
   1.1 Review of RERTR Mini-plate Test Design 1
   1.2 Description of the RERTR-10 Test 1
   1.3 Results 3

2. RERTR-10A PLATE L1P145 FAILURE ANALYSIS 7
   2.1 In-Canal Examination 7
   2.2 Non-Destructive Examination of Breached Plate 7
   2.3 Destructive Examination 9
   2.4 Oxide Formation 10
      2.4.1 Boehmite Layer Formation 10
      2.4.2 Boehmite Layer Defect Mechanisms 12

3. FUEL PLATE DELAMINATIONS 14
   3.1 As-Fabricated Delaminations (Fuel/Clad Debonds) 14
      3.1.1 Behavior of Design Debonds in HIP Mini-plates 14
      3.1.2 RERTR-12 Blister Anneal Summary 26
   3.2 Delaminations Due to Fuel Performance 27
   3.3 Mitigations for Fuel/Clad Bond Defects 30

4. SUMMARY 31

FIGURES

Figure 1. RERTR mini-plate. 1

Figure 2. RERTR mini-plate capsule. 2

Figure 3. Cross section of irradiated mini-plate. The arrows indicate the area of maximum fuel/clad interfacial stress due to large edge swelling and the type of interfacial phenomena of interest. 2

Figure 4. RERTR-10A average fuel plate swelling. 4

Figure 5. Photographs of the several fuel plates from the RERTR-10A test. (a) L1P145 – silicon-modified (note discoloration on lower edge of plate over the delamination, note blister at bottom of plate), (b) L1P202 – silicon-modified (note discoloration on lower edge of plate over the delamination), and (c) L1P12Z – Zr barrier. 5

Figure 6. Metallographic cross sections taken from the mid-plane of the (a) L1P145 – silicon-modified and (b) L1P12Z – Zr barrier fuel plates. The images show the cracking and delamination that occurred in the silicon-modified plate compared to the Zr barrier plate. 6

Figure 7. Higher magnification image of the metallographic cross section of the L1P12Z – Zr barrier fuel plate. 6

Figure 8. Front and back side photographs of the RERTR-10A fuel plate L1P145 before irradiation. 7

Figure 9. Front and back side photographs of the RERTR-10A fuel plate L1P145 after irradiation. Coolant flow was from the left to right during irradiation. 8

Figure 10. Fuel plate image showing the blister, rupture point, and surface oxide irregularity 8

Figure 11. Fuel plate sectioning diagram. 9

Figure 12. Transverse cross section of blister. 9

Figure 13. Axial cross section of blister. 9

Figure 14. Boehmite formation. 10

Figure 15. Micropitting in boehmite fuel cladding. 11

Figure 16. Pitting corrosion observed in RERTR-1 fuel plate. Fuel plates were not pre-filmed prior to irradiation. 13

Figure 17. Layup of Grafoil, (a) beneath U-Mo foil and (b) in Al-Al interface. 15

Figure 18. Layup of Ta foil (all are double thickness). 16

Figure 19. Yttria applied to cover plate. 16

Figure 20. Oxide regions on cover plate. 17

Figure 21. Polyimide film on Al plate. 17

Figure 22. Control plate. (a) as-HIPed, (b) blister annealed (no blisters noted), (c) UT scan of annealed plate. 19

Figure 23. Yttria coated plate. (a) as-HIPed, (b) blister annealed (two blisters noted), (c) UT scan of annealed plate. 20

Figure 24. Anodized plate. (a) as-HIPed, (b) blister annealed (no blisters noted), (c) UT scan of annealed plate. 21

Figure 25. Tantalum foil plate. (a) as-HIPed, (b) blister annealed (no blisters noted), (c) UT scan of annealed plate 22

Figure 26. Grafoil foil plate. (a) as-HIPed, (b) blister annealed (blisters marked), (c) blister annealed (obverse—blisters noted), (d) UT scan of annealed plate. 23

Figure 27. Polyimide film plate. (a) as-HIPed, (b) blister annealed (blisters marked), (c) blister annealed (obverse—blisters noted), and (d) UT scan of annealed plate. 24

Figure 28. Photographs of the several fuel plates from the RERTR-10A test. (a) L1P145 – silicon-modified (note discoloration on lower edge of plate over the delamination, note blister at bottom of plate), (b) L1P202 – silicon-modified (note discoloration on lower edge of plate over the delamination), and (c) L1P12Z – Zr barrier. 28

Figure 29. Neutron radiographs of the three fuel plates shown in Figure 28. Note that for the silicon-modified plates, the internal cracks in the foil coincide with the delaminations and surface discoloration observed on the surface. It is also significant that cracking is not observed in the Zr barrier fuel plate. 29

Figure 30. Metallographic cross sections taken from the mid-plane of the three fuel plates shown in Figure 28. The images show a significant difference in the extent of cracking that occurred in the silicon modified plates compared to the Zr barrier plate. 30

TABLES

Table 1. Description of RERTR-10A test design. Each entry describes the material added to modify the fuel/clad interface chemistry. The A and C capsule compositions were identical..... 3

Table 2. Description of RERTR-10B test design. Each entry describes the material added to modify the fuel/clad interface chemistry. The B and D capsule compositions were identical except that the niobium barrier is replaced with a second Zr barrier plate in the D capsule. 3

Table 3. Design debond HIP run. 15

Table 4. Comparison of debond test results. 25

ACRONYMS

ATR	Advanced Test Reactor
B&W	Babcock and Wilcox
BFFL	Boosted Fast Flux Loop
FASB	Fuels and Applied Science Building
FB	friction bonding
HFEF	Hot Fuel Examination Facility
HIP	hot isostatic pressing
HTF	Hydraulic Test Facility
MTR	Materials Test Reactor
PIE	post irradiation examination
R&D	research and development
RERTR	Reduced Enrichment for Research and Test Reactors
UT	ultrasonic testing
VDC	volt DC

RERTR-10A Test: Overview and Breach Assessment

1. DESCRIPTION OF THE RERTR-10A TEST

The Reduced Enrichment Research and Test Reactor (RERTR) program has been working to develop a very high density nuclear fuel for research and test reactors based on uranium-molybdenum alloys for the last decade. Over the course of that development, the program has conducted 15 irradiation campaigns in the Advanced Test Reactor (ATR) (in addition to collaborating with several foreign irradiation programs). The testing sequence includes initial tests that focus on very small scale samples used to screen materials (micro-plates), small scale samples to test specific fuel performance phenomena and to develop fabrication techniques (mini-plates), full-size plates to demonstrate fabrication technology and explore integrated fuel performance properties, and full elements to demonstrate performance.

1.1 Review of RERTR Mini-plate Test Design

The RERTR mini-plate test trains consist of 32 mini-plates assembled into four capsules (eight mini-plates per capsule). Not all mini-plates contain fuel. Schematics of a plate and capsule are shown in Figures 1 and 2. The capsules are stacked vertically in a basket, which is inserted into an ATR Large B position in the reflector region. To achieve the desired test conditions, the capsules are cooled by direct contact with ATR primary coolant. Each mini-plate fuel meat contains approximately 6 grams of uranium. Currently, 321 fuel plates have been tested in the ATR as part of the RERTR program.

1.2 Description of the RERTR-10 Test

The RERTR program has worked over the last decade to develop an understanding of how uranium-molybdenum alloys behave under irradiation. It is clear from these studies that the fuel behaves in a stable, predictable manner with modest swelling to very high burnup. Breakaway swelling in the fuel phase is extremely unlikely to occur under typical Materials Test Reactor (MTR) conditions. Monolithic fuel performance research is currently focused on optimization of the fuel/clad interface. This interface may deteriorate throughout irradiation due to the formation of undesirable U-Mo/Al reaction products. The RERTR-10 mini-plate test was designed to evaluate the performance of several different modifications to this interfacial layer.

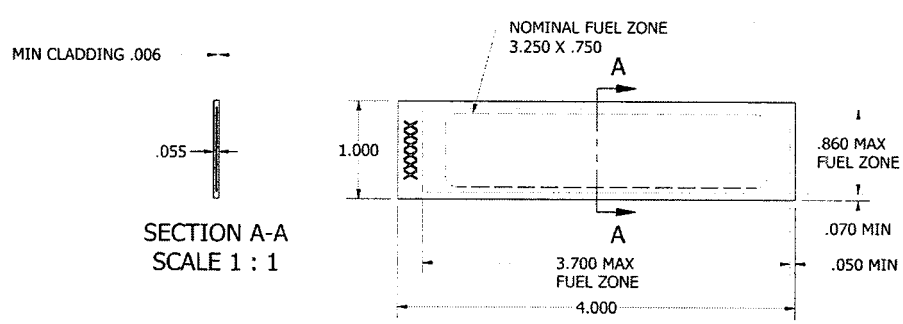

Figure 1. RERTR mini-plate.

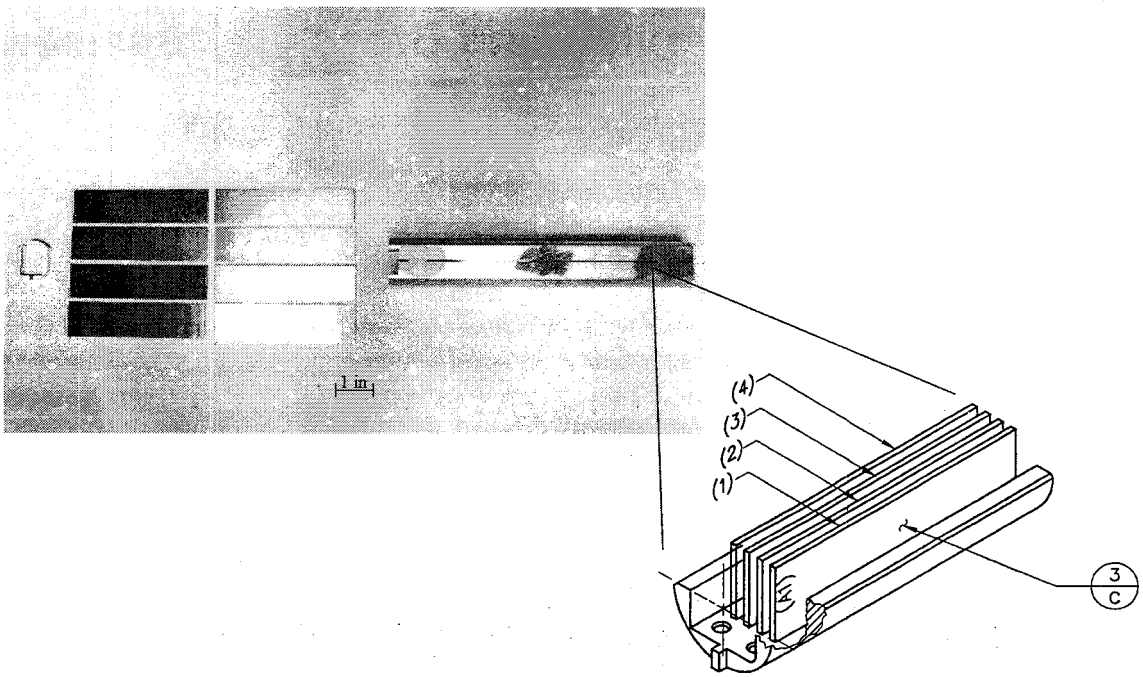

Figure 2. RERTR mini-plate capsule.

To observe performance behaviors that differentiate these fuel designs, the fuel plates must be irradiated to high burnup (> ~100% LEU equivalent) and the fuel/clad interface must be subjected to tensile forces during irradiation. The RERTR-10 mini-plate test was consequently oriented perpendicular to the neutron flux gradient such that the inner edge of the plate experiences larger fission densities (and thus swelling) than the outer edge. At the end of irradiation the differential swelling that occurs between the two edges results in a tensile load at the fuel/clad interface. The force is maximized locally at the location shown in Figure 3.

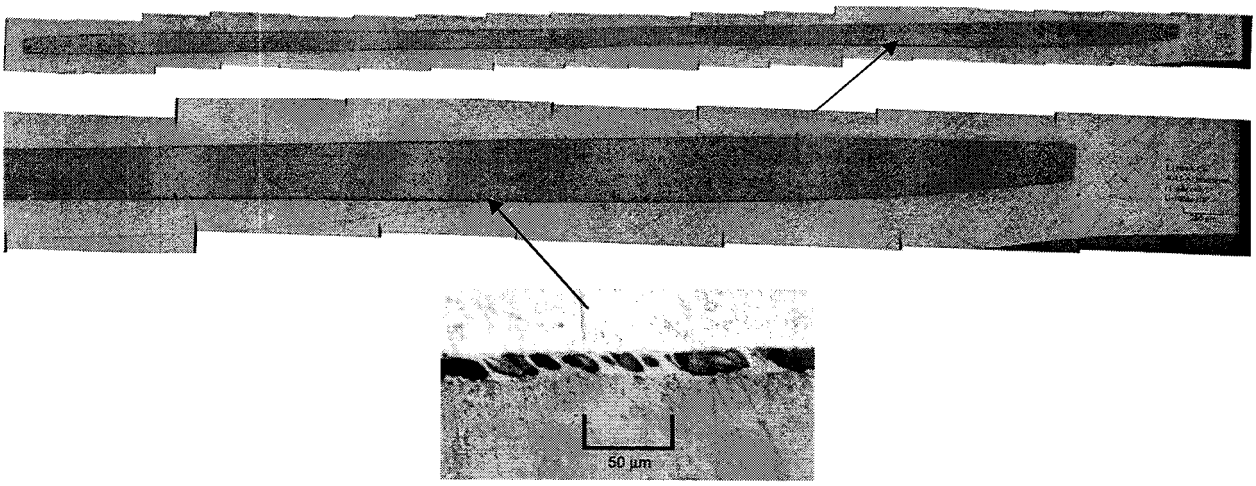

Figure 3. Cross section of irradiated mini-plate. The arrows indicate the area of maximum fuel/clad interfacial stress due to large edge swelling and the type of interfacial phenomena of interest.

The RERTR-10 test was split into two campaigns: RERTR-10A and RERTR-10B. The RERTR-10A test was fabricated by hot isostatic pressing (HIP) and utilized the A and C capsules in the RERTR-10 irradiation basket. The RERTR-10A test matrix is shown in Table 1. The RERTR-10B test was fabricated by friction bonding (FB) and utilized the B and D capsules of the RERTR-10 irradiation basket. The RERTR-10B test matrix is shown in Table 2. The RERTR-10A test was completed first and began irradiation in ATR Cycle 142B. The RERTR-10B positions in the irradiation basket were filled with non-fueled 'blank' capsules during Cycle 142B. The RERTR-10B capsules were inserted for ATR Cycle 143A.

A cladding breach was identified on the RERTR-10A test during Cycle 143A and was subsequently removed from the reactor. The RERTR-10B test was reinserted to complete the irradiation cycle. Although an additional cycle of irradiation was planned, the RERTR-10B test was terminated at this point.

Table 1. Description of RERTR-10A test design. Each entry describes the material added to modify the fuel/clad interface chemistry. The A and C capsule compositions were identical.

RERTR-10A	A1 (L1P30Z)/ C1 (L1P12Z)	A2 (L1P256)/ C2 (L1P266)	A3 (L2P15Z)/ C3 (L2P16Z)	A4(L1P135)/ C4 (L1P145)
First side	Zirconium	Al-12 Si alloy	Zirconium	Al-2 Si alloy
Second side	Zirconium	Al-12 Si alloy	Zirconium	Al-2 Si alloy
	A5 (L1P234)/ C5 (L1P244)	A6 (L1P213)/ C6 (L1P223)	A7 (L1P192)/ C7 (L1P202)	A8 (L1P171)/ C8 (L1P181)
First side	Al-3.5 Si blend	Al+1.5 Si blend	Al+0 Si blend	Thin Si
Second side	Al+5 Si blend	Al+2 Si blend	Al+1 Si blend	Thick Si

Table 2. Description of RERTR-10B test design. Each entry describes the material added to modify the fuel/clad interface chemistry. The B and D capsule compositions were identical except that the niobium barrier is replaced with a second Zr barrier plate in the D capsule.

RERTR-10B	B1 (Dummy)/ D1 (Dummy)	B2 (L1F401)/ D2 (L1F381)	B3 (L1F417)	D3 (L1F427)	B4 (Dummy)/ D4 (Dummy)
First side	–	Thin Si	Thin Si	Thin Si	–
Second side	–	Thick Si	Thick Si	Thick Si	–
	B5 (Dummy)/ D5 (Dummy)	B6 (L2F46Z)/ D6 (L2F45Z)	B7 (L1F44N)	D7 (L2F47Z)	B8 (Dummy)/ D8 (Dummy)
First side	–	Zirconium	Niobium	Zirconium	–
Second side	–	Zirconium	Niobium	Zirconium	–

1.3 Results

Post irradiation examination (PIE) was conducted on the plates irradiated in the RERTR-10A fuel test to compare the relative performance of the Zr and silicon-modified interface monolithic fuel designs. It was previously demonstrated that the U-Mo fuel phase had performed exceptionally well in all tests to very high burnup (INL/EXT-07-13271, "RERTR-7 PIE Letter Report"). Therefore, the examination was focused on evaluation of the fuel/clad interface layer performance.

Non-destructive examination of the fuel plates clearly showed that the fuel plates with a silicon-modified interface experienced significantly greater swelling than the Zr barrier fuel plates. In some cases the degree of swelling indicated a delamination inside the fuel plate (Figure 4).

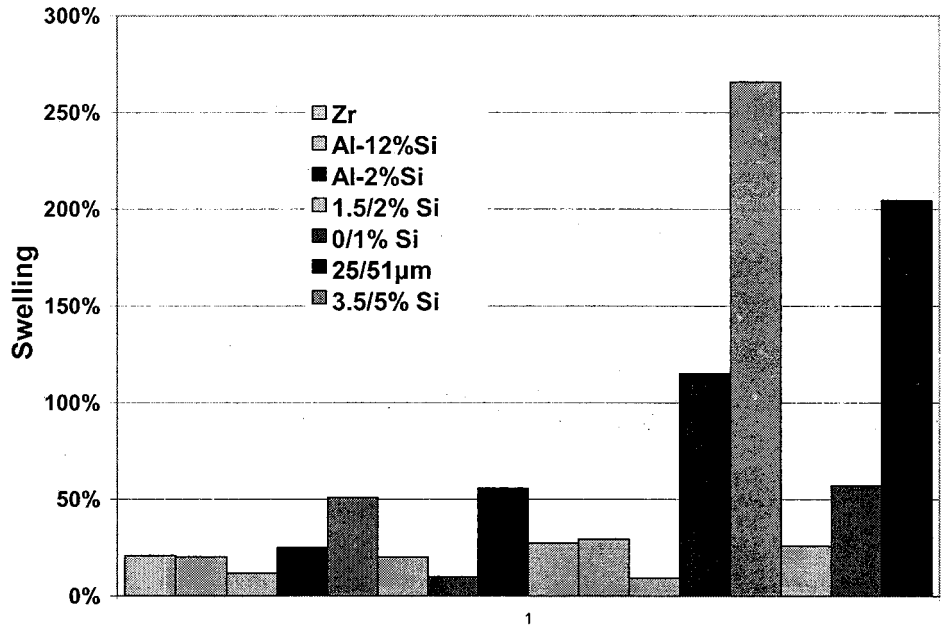

Figure 4. RERTR-10A average fuel plate swelling.

Several fuel plates were sectioned for metallographic examination of the fuel/clad interface. These cross sections clearly showed the difference in mechanical stability between the Zr barrier interface and the silicon-modified interface. Photographs of fuel plates from the RERTR-10A test are shown in Figures 5, 6, and 7. All of the silicon-modified fuel plates were either delaminated prior to cutting or delaminated during cutting. Conversely, no delaminations were observed in the Zr barrier fuel plates. There are no indications that the material in the fuel/clad layer of the Zr barrier system is being meaningfully degraded by irradiation to very high burnup. It is also significant that while all the plates examined contained fuel foil cracking due to the extreme mechanical stresses applied to the fuel plate during operation or during cutting of the plate, the nature and extent of cracking in the Zr fuel plates was significantly less severe than in the silicon-modified plates.

It is important to highlight that the breached fuel plate in the RERTR-10A test was a silicon-modified fuel plate. This fuel plate will be discussed in greater detail in Section 2.

Based on these observations, the Zr barrier-based fuel design has been selected for future testing. The silicon-modified design has been dropped from further testing.

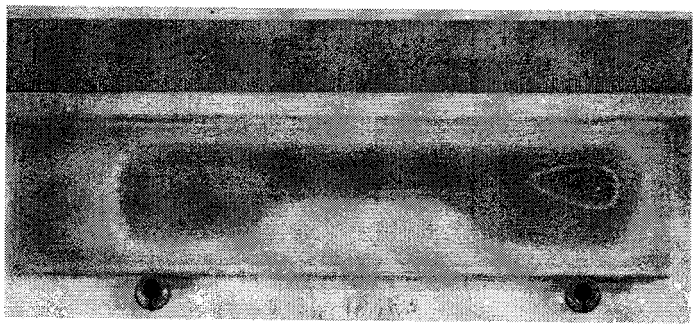

(a)

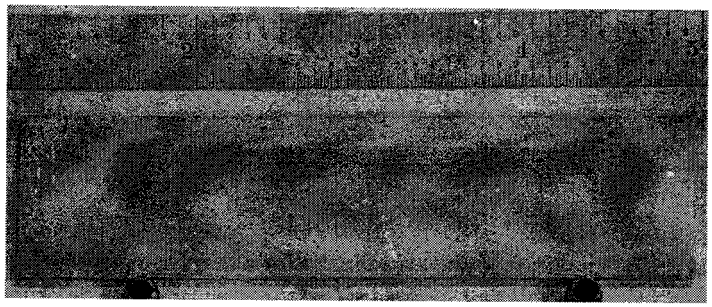

(b)

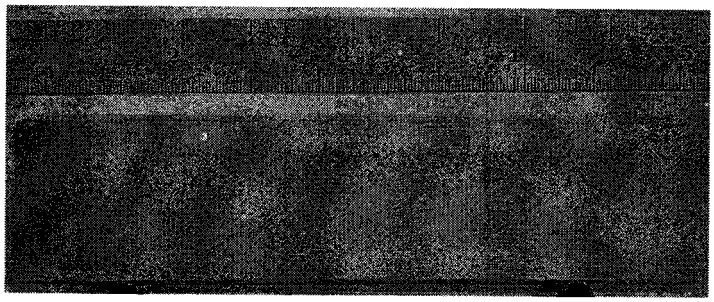

(c)

Figure 5. Photographs of the several fuel plates from the RERTR-10A test. (a) L1P145 – silicon-modified (note discoloration on lower edge of plate over the delamination, note blister at bottom of plate), (b) L1P202 – silicon-modified (note discoloration on lower edge of plate over the delamination), and (c) L1P12Z – Zr barrier.

(a)

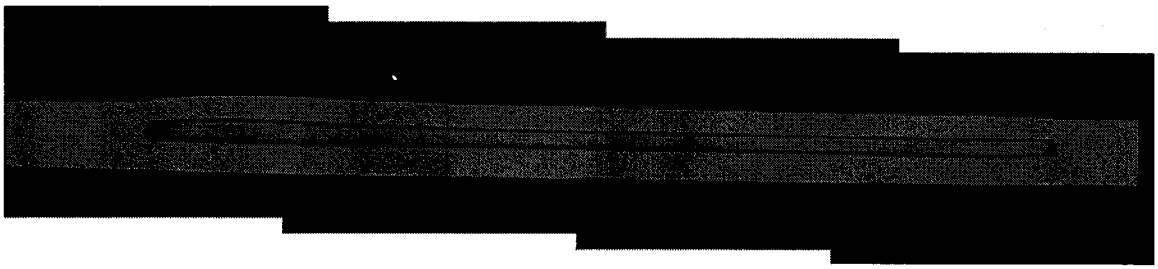

(b)

Figure 6. Metallographic cross sections taken from the mid-plane of the (a) L1P145 – silicon-modified and (b) L1P12Z – Zr barrier fuel plates. The images show the cracking and delamination that occurred in the silicon-modified plate compared to the Zr barrier plate.

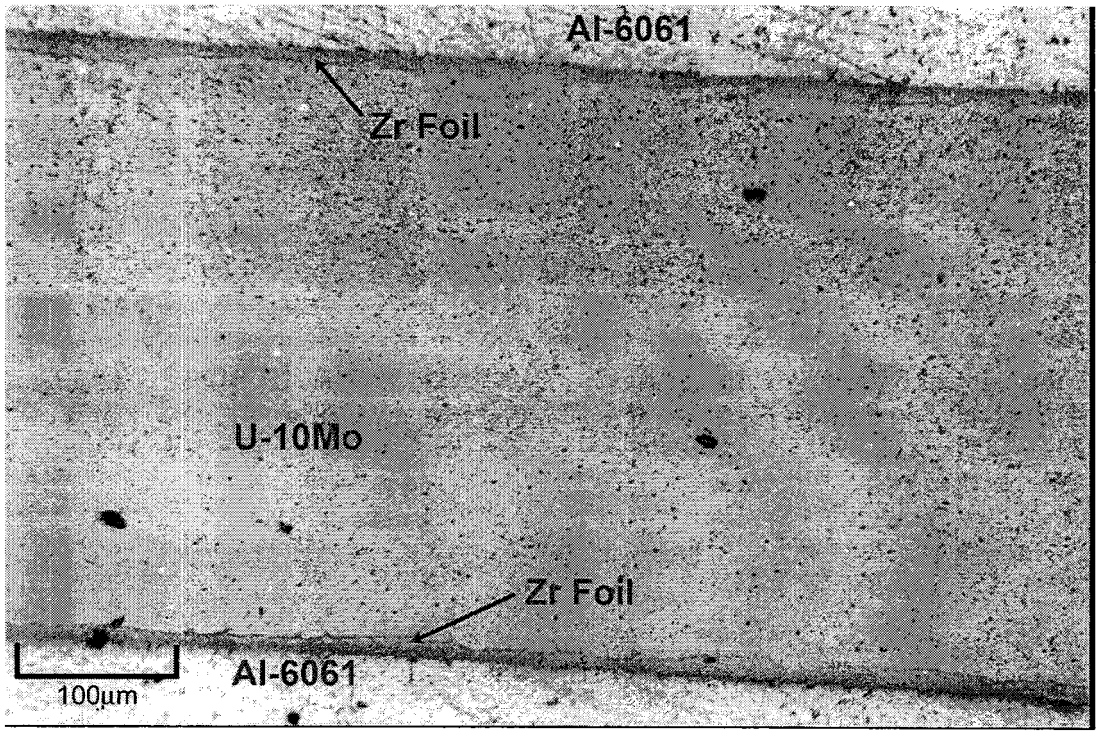

Figure 7. Higher magnification image of the metallographic cross section of the L1P12Z – Zr barrier fuel plate.

2. RERTR-10A PLATE L1P145 FAILURE ANALYSIS

Additional study of the breached fuel plate was conducted to evaluate the failure mode and to make informed updates to the fuel design and/or fuel specifications. The failure mode was identified and process modifications were recommended. Considerations to augment the assessment of a second potential failure mode were also proposed.

2.1 In-Canal Examination

The RERTR-10A test capsules were examined in the ATR canal December 8, 2008 in an effort to identify the source of fission product release observed during irradiation in ATR Cycle 143A. The capsules were back-lit through the coolant channels in an effort to identify any abnormal plate growth. This information is, at best, qualitative but can give indications of non-typical behavior. As expected, fuel plates in Capsule A showed very little swelling (due to the low burnup) while fuel plates in Capsule C showed visible swelling consistent with previous experience. However, one plate in Capsule C did appear to have developed a blister on one side of the fuel plate.

2.2 Non-Destructive Examination of Breached Plate

Following transport to the Hot Fuel Examination Facility (HFEF), the capsules were dismantled and all 16 plates were visually examined. Plate L1P145, located in Position C4, showed the presence of a surface blister on the front of the plate (as was observed during in-canal observation) with a clear rupture point. The remaining 15 plates showed no abnormal features. Photographs of fuel plate L1P145 before and after irradiation are shown in Figures 8 and 9, respectively.

A higher magnification image of the blister is shown in Figure 10. The blister size is roughly ¼ inch by ½ inch in size (approximately half the size of a dime).

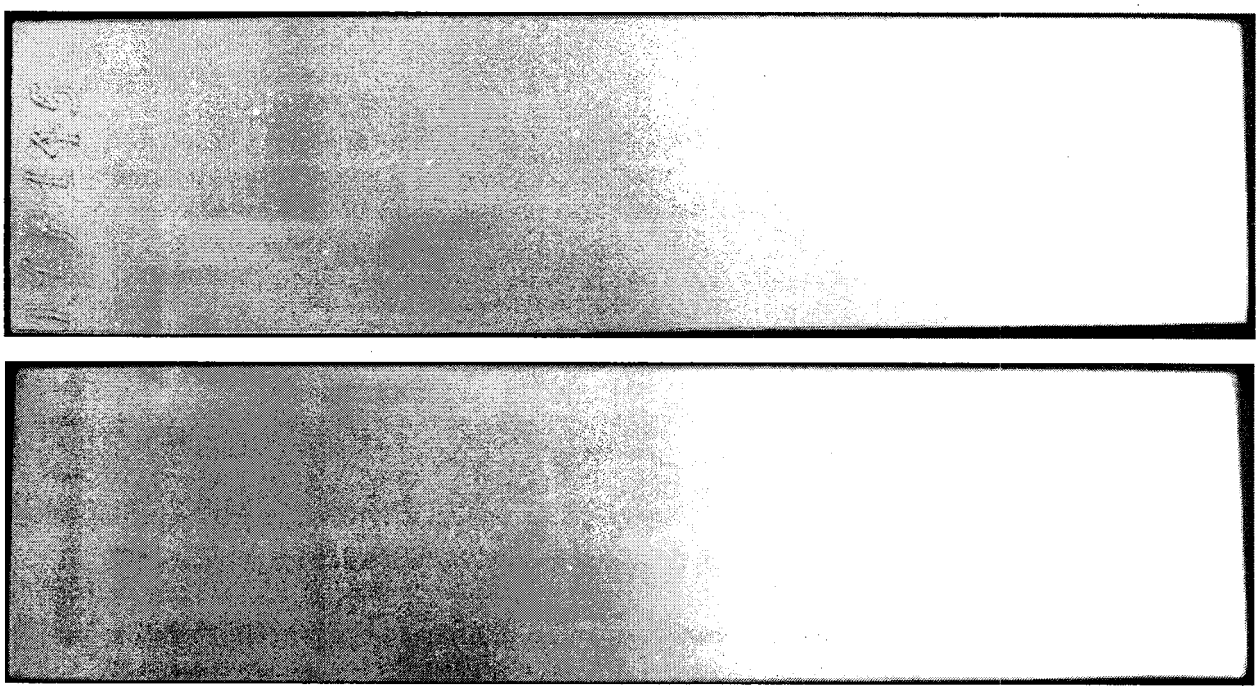

Figure 8. Front and back side photographs of the RERTR-10A fuel plate L1P145 before irradiation.

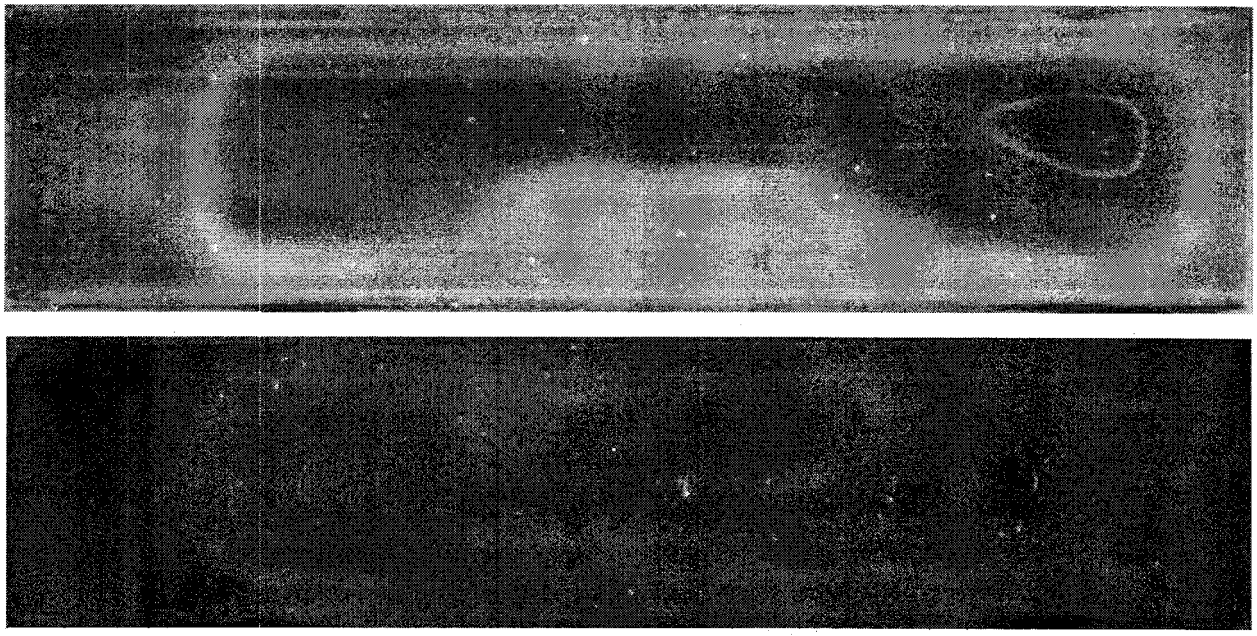

Figure 9. Front and back side photographs of the RERTR-10A fuel plate L1P145 after irradiation. Coolant flow was from the left to right during irradiation.

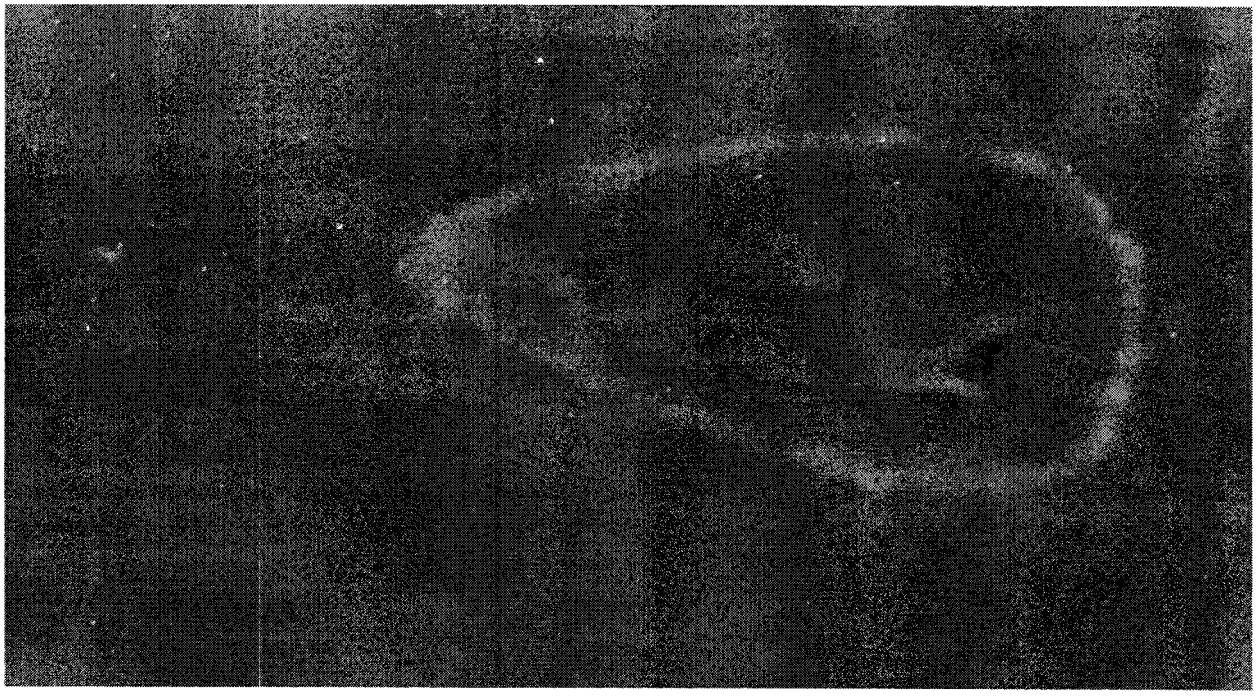

Figure 10. Fuel plate image showing the blister, rupture point, and surface oxide irregularity

Additional examination was performed (gamma scanning, neutron radiography, and thickness measurement) and the only other anomaly identified was a crack inside the fuel foil revealed in the neutron radiograph. Both the gamma scanning and neutron radiography showed that very little fuel or fission product inventory was lost through the blister.

2.3 Destructive Examination

Two sections were taken from the blistered region for metallographic examination, as shown in Figure 11. The images from these two mounts are shown in Figures 12 and 13.

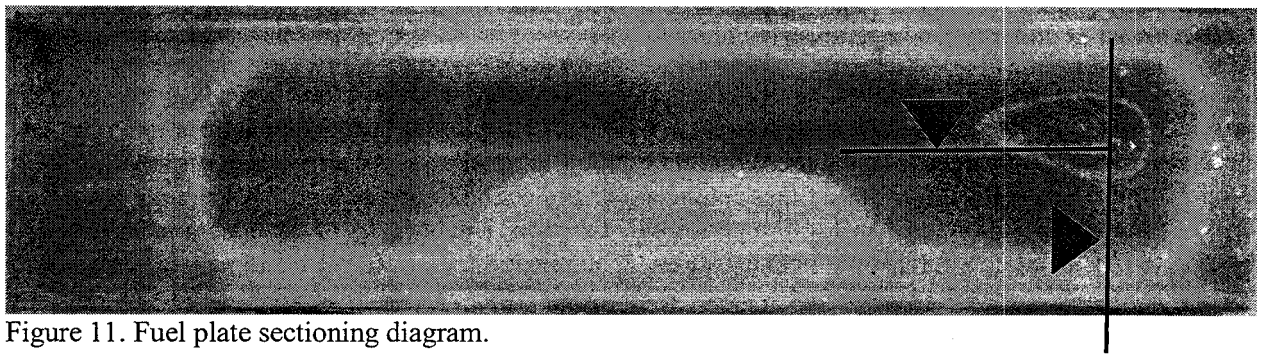

Figure 11. Fuel plate sectioning diagram.

Figure 12. Transverse cross section of blister.

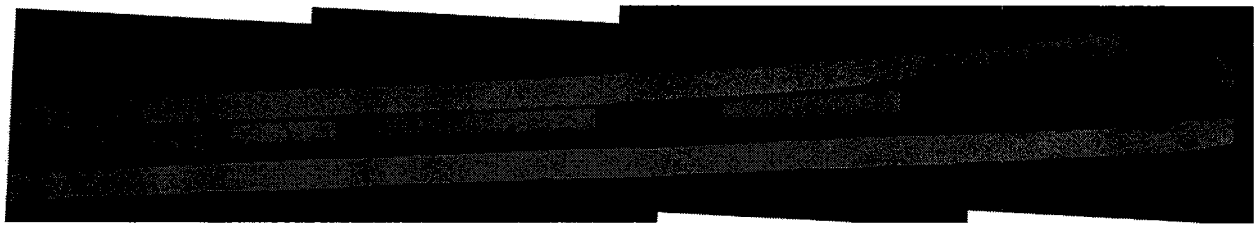

Figure 13. Axial cross section of blister.

Both cross sections show the presence of a very thick (~300 μm) layer of Al oxide over the top of the blistered area. Typical oxide layer thicknesses are in the range of 10 μm. The extremely low thermal conductivity of the oxide material results in a substantial increase in cladding temperature underneath the oxide. The presence of this oxide layer would reduce the mechanical strength of the cladding, encourage clad buckling through thermal expansion, and enhance fission gas release from the fuel region under the oxide layer. Ultimately, these three phenomena combined to cause the fuel plate blister. Formation of cracks in the cladding material, due to the mechanical deformation experienced during blistering, would result in fission gas release from the fuel plate.

It is clear that the root cause of the breach is the formation of the thick oxide layer, which led to formation of the blister on the fuel plate surface.

2.4 Oxide Formation

Oxide formation on the surface of Al clad fuel plates is a well known phenomenon. It has been demonstrated that the rate of corrosion is strongly dependent on the Al surface temperature and the composition of the oxide layer. It has been observed many times in the ATR that cladding corrosion can lead to breaches under typical operating conditions.

Protection of the ATR cladding material from excessive oxidation during irradiation is currently provided by a fully aged continuous boehmite layer that is created through autoclaving prior to irradiation. When fully aged, boehmite is a thermally stable crystalline surface film under irradiation. Proper application of this layer during fabrication and its protection during subsequent handling are critical prior to irradiation in order for it to perform its function. The integrity of the boehmite layer can be affected by its processing history, damage and/or contamination, or defective cladding.

2.4.1 Boehmite Layer Formation

Aluminum metal in contact with water initially forms an amorphous ionic-ring gelatinous solid with an approximate chemical form of:

$Al_6(OH)_{12}^{6+}\ 12H_2O$

Through deprotonation and condensation reactions, hexagonal chains or rings of polynuclear complexes form, which continue their deprotonation and condensation sequence to first become a gelatinous boehmite.

The gelatinous boehmite then continues to age to a fully crystalline solid (see simplified Figure 14) on the basis of the temperature, pressure, and pH of the system.[a] This sequence on the surface of Al at room temperature takes many hours, with gelatinous boehmite forming within about four hours, and a fully crystalline solid hydroxide being present after more than 16 hours of exposure. "Aging" is the generalized term to summarize the polycondensation of a gelatinous precipitate to become a structurally ordered and thermodynamically defined compound (i.e., crystalline boehmite).

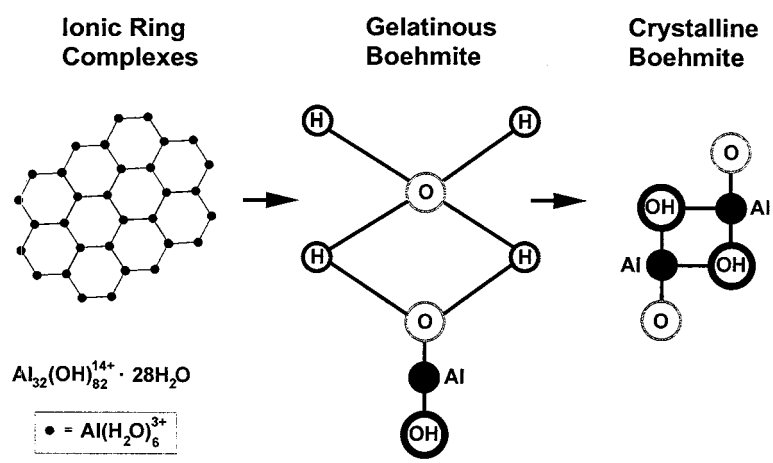

Figure 14. Boehmite formation.

a. Wefers, K. and Misra, C., "Oxides and Hydroxides of Aluminum," Alcoa Technical Paper No. 19, Revised, Alcoa Laboratories, 1987.

Formation of crystalline boehmite requires a pH above 4.8, an autoclave temperature above 105°C and sufficient time to age the structure. Historically, shorter processes (typically 4 hours at 185°C) have been used on the basis that aging will occur more rapidly at the higher temperature, if the water is not contaminated with carbonates or other ionic species that retard the aging process.

Boehmite aging is essential for achieving full layer passivation in reactor service. Boehmite will not passivate under exposure to high radiation fields, so it is essential to have the layer fully aged and passive before insertion in the reactor.

Physical damage of boehmite is always a possibility during plate assembly. The probability of layer damage, however, increases rapidly for boehmite that is not completely aged. Such boehmite coatings will be much softer and more easily scratched than fully aged material.

Non-uniformity in the boehmite layer thickness typically results from two causes, only one of which is preventable with this specific alloy (AA6061-O). The preventable cause is attempted autoclaving of the Al at the low pH end of the boehmite passivation region (at a pH around 4.8). At this pH the boehmite is trying to form at the same time some Al is going into solution as Al^{+3} ion so the pH of the autoclave is very difficult to control and as the pH fluctuates to the high side, the Al^{+3} will tend to precipitate out in various locations as gelatinous boehmite on fuel surfaces. This issue results in a spotty or sometimes layered boehmite that is typically not fully aged since it was being formed, dissolved, and re-formed throughout the autoclaving process.

The non-preventable non-uniformity in boehmite applied to AA6061-O fuel cladding is from the growth of boehmite around surface connected second phase particles in the alloy. This alloy contains Si, Mg, Fe, and Cu that form a variety of relatively large interstitial particles during fuel annealing steps. When the hydroxide grows around these particles, micropits are effectively formed along the surface of the cladding many times the thickness of the nominal boehmite surface layer, often dissolving or redistributing the second phase particle depending on composition (see Figure 15).

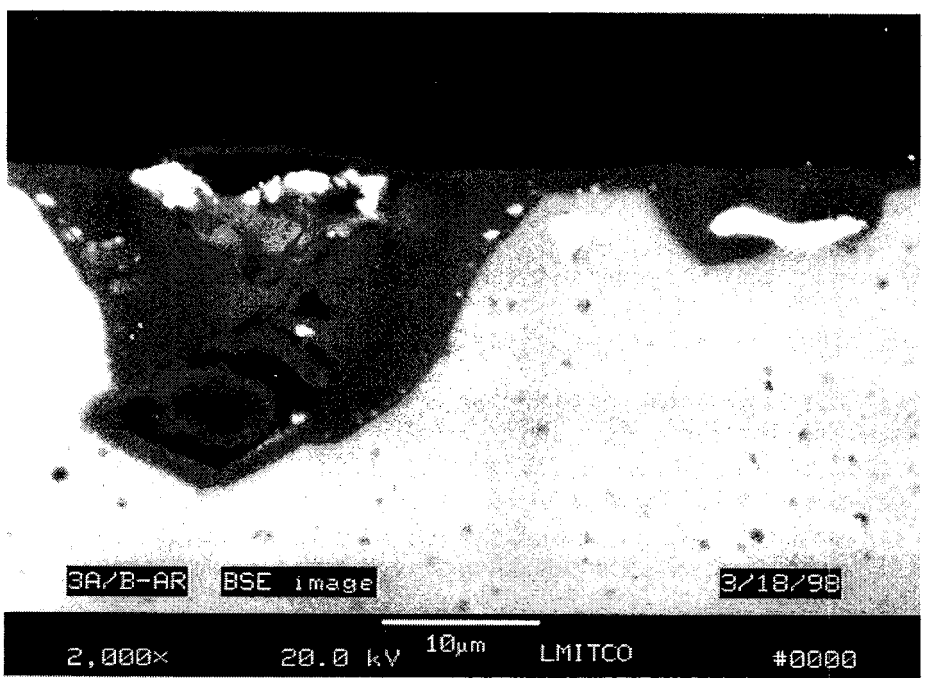

Figure 15. Micropitting in boehmite fuel cladding.

2.4.2 Boehmite Layer Defect Mechanisms

Several different potential cladding oxidation defect modes were examined. The probability of each defect type and potential mitigations for each were considered.

2.4.2.1 Autoclaving to Achieve the Boehmite Layer

A successful, science-based autoclaving process was developed for the ATR fuel when the process was moved to the fuel manufacturer (Babcock and Wilcox [B&W]) in the mid 1990s. This process requires autoclaving for a minimum of 18 hours at 185°C and a pH above 5.0 to achieve a specified hydroxide layer thickness on ATR fuel elements. Shortcuts to this proven process should be undertaken only by those fully familiar with the formation chemistry and aging behavior involved. Non-uniformity due to hydroxide dissolution and re-formation sequences will not occur if an appropriate autoclave process is used.

However, during review of the RERTR autoclaving process it was identified that the program was implementing a process supplied by ATR early in the program that was based on the Hydraulic Test Facility (HTF) process. (Soak at 185°C in deionized water for 4 hours). It is believed that following this process would not provide the same level of protection as the B&W process (soak at 185°C in deionized water with pH of 8.0 for 18 hours). This process was previously demonstrated for the Boosted Fast Flux Loop (BFFL) Experiment in ATR and will be implemented in future RERTR tests.

2.4.2.2 Micro-Pitting Non-Uniformity in Layer Thickness

Micro-pitting behavior has been accepted in ATR fuel cladding since usage of Al-6061 alloy began and could only be prevented by changing back to a pure Al. Usage of the Al-6061alloy was started to provide additional structural strength in the fuel element assembly (especially for the crimped joint between fuel plates and frame), and to have the entire assembly constructed from the same material.

2.4.2.3 Defective Cladding Material

Fuel cladding sheet is the result of alloying Al with the required alloying elements in the molten state, casting, and forming to the required final gage thickness. The casting and forming processes, which typically include a minimum of one cross rolling step, are expected to break up and fully disperse alloying elements that are not already in solid solution in the alloy. Defective cladding material could be caused by an incomplete break up or dispersion of alloying elements, or by the presence of some other localized contaminant. However, correction of this type of rare defect would require basic changes to the casting and forming schedule for the parent material, which could only be done at great expense.

2.4.2.4 Contamination or Damage of the External Cladding Surface

A review of fabrication processes was conducted, including the cladding procurement, the cleaning, handling, and inspection processes, and a comparison with industry standard practices. The review showed that the Al (Al-6061 alloy) was procured at Quality Level 2 from an approved supplier with material certifications. In addition, the material was sent to an approved laboratory for independent certification. The next step of the review showed that proper handling, cleaning, and inspection was performed in the Fuels and Applied Science Building (FASB) fuel plate fabrication, especially in the critical steps before the HIP. The procedures and activity sheets used to track fabrication are comparable to those used at B&W in fabricating dispersion fuel plates, and match industry standard practices. During the review, several best practices were noticed, which were not required or documented in the procedure. To ensure their continuation, the procedure and activity sheets were updated to emphasize these best practices.

2.4.2.5 Accelerated Oxide Growth

ATR conditions can result in significant corrosion even at low temperature. Oxide growth rate under irradiation is well-known to be tightly coupled to the surface temperature of the cladding. It has been observed that typical ATR coolant conditions are sufficient to cause pitting corrosion without a complete boehmite layer. Defects similar to the 10A were also seen in the RERTR-1 and 2 tests (see Figure 16) before pre-filming was implemented. This sensitivity would be enhanced further by high operating temperature.

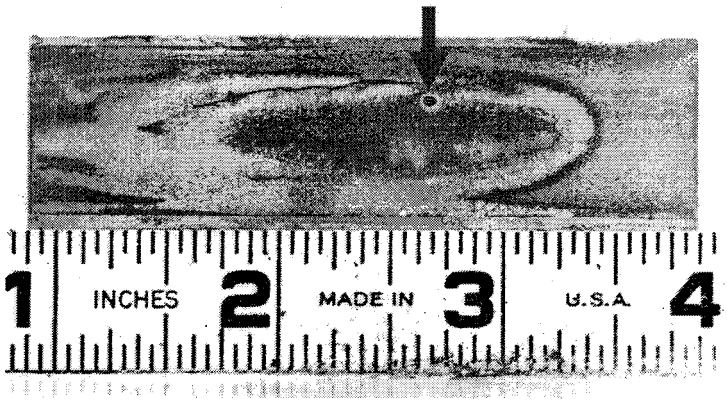

Figure 16. Pitting corrosion observed in RERTR-1 fuel plate. Fuel plates were not pre-filmed prior to irradiation.

2.4.2.6 Summary of Corrosion Observations

Review of the failure mechanism for plate L1P145 showed that the root cause of failure was excessive surface corrosion in a localized area. Examination of several root causes suggests that the defect can be attributed to incomplete aging of the boehmite applied prior to irradiation. This process has been modified to ensure proper boehmite aging, which will provide better oxide protection for future experiments.

3. FUEL PLATE DELAMINATIONS

It can be postulated that an increase in surface temperature is possible due to delamination between the fuel and cladding that could impact surface oxidation rates. A delamination would affect the heat flow, resulting in a non-uniform heat distribution. The gas gap created by the delamination would reduce the heat transfer from that side of the plate, resulting in higher surface clad temperatures on one side of the plate than the other (approximately a 40°C difference). Delaminations can occur either before irradiation (as-fabricated) or during irradiation (irradiation induced). Observations and studies conducted to examine and mitigate the impact of those features in future experiments are outlined in the following sections.

3.1 As-Fabricated Delaminations (Fuel/Clad Debonds)

An assessment was performed to evaluate if pre-existing defects may have gone unidentified during the pre-irradiation fuel plate scanning. This review included examination of traditional techniques applied to identify as-fabricated debonds (blister anneal) to determine if they are appropriate for the monolithic fuel design. A generic study of delamination identification in monolithic fuel using the blister anneal and UT scanning process and a summary of observations made during the examination of mini-plates manufactured for the RERTR-12 test are presented.

3.1.1 Behavior of Design Debonds in HIP Mini-plates

3.1.1.1 Introduction

In order to further characterize the effect of debonds and the different analysis methods that are currently used on finished fuel plates, a test was conducted where debonding agents were deliberately introduced into surrogate plates as part of a HIP run.

3.1.1.2 Current Debond Testing

Currently, a total of three types of tests are done on the finished fuel plates to measure debonding as part of qualification for reactor insertion: (1) ultrasonic, (2) blister, (3) bend. Of the three, only UT is a true "nondestructive" test.[b] UT uses transmitted sound waves to measure attenuation of sound transmitted through the plates. Blister annealing subjects the plates to elevated temperatures (typically 475–500°C) for a length of time. Any contaminants that outgas at the blistering temperature or air pockets where the trapped gas can expand can cause the surface of the plate to form an elevated region, called a "blister." The heating cycle comprising of a blister anneal is part of the thermal history of a fabricated plate, and at a minimum, changes the microstructure of a processed plate. Bend testing is a destructive analysis, but for the purposes of fuel qualification it does not alter the final fuel plate as the test is conducted on the adjacent material removed from the plate during processing. The samples are bent back and forth and the interface is examined for signs of delamination, which indicates a failure.

3.1.1.3 Test Description

Over the course of the RERTR monolithic testing, the HIP process has shown to be a robust fabrication method with very few defects detected by the testing methods mentioned above. In order to have quantifiable debond regions, a series of contaminants were introduced. The tests were conducted in HIP Run 63 comprised of Plates 63-1–63-6 (Table 3).

---

b. Non destructive testing is defined here as a test that does not destroy or permanently alter the material being tested

Table 3. Design debond HIP run.

ID	Contaminant	Debond Method	Applied to	Cleaning
63-1	Hydrocarbon	Polyimide film	On interface surface during layup	Chemical
63-2	Carbon—Grafoil®	Cut foils	On interface surface during layup	Chemical
63-3	Metal Foil—Ta	Cut foils (double thickness)	On interface surface during layup	Chemical
63-4	Oxide	Anodized over whole plate	On cover plate	Selective wire brush
63-5	Yttria—aerosol	Mask (blue painter's tape) and paint	On cover plate	Chemical
63-6	None—Control	N/A	N/A	Chemical

Of six plates in Run 63, one plate was introduced as an unaltered control, and four plates had regions of differing "inert" material introduced at the interface: graphite, tantalum, yttrium oxide, and Al oxide selected to simulate a range of defect types (graphite–contamination, tantalum–folds in foil, yttrium–disposed porous material, Al oxide–incomplete cleaning, polymeric film–outgassing). The final plate used a polymeric material designed to break down and outgas during the process. Each inert material used is described in further detail below.

The graphite was in the form of a flexible graphite foil Grafoil®,[c] which is currently used in the HIP process as a barrier to keep the plates from bonding with the HIP can, the strongbacks, or each other. This grade of Grafoil contains a high percentage (99.8%) of carbon and does have some inherent porosity. This material was cut from a 0.005-in.-thick sheet in the shape of small squares. The materials used in the HIP run measured (nominally, on the square) 1 cm, 0.75 cm, 0.5 cm, 0.25 cm, 0.125 cm, and .0125 cm. The squares were placed both under the foil and on the interface between the two Al cladding sheets (Figure 17).

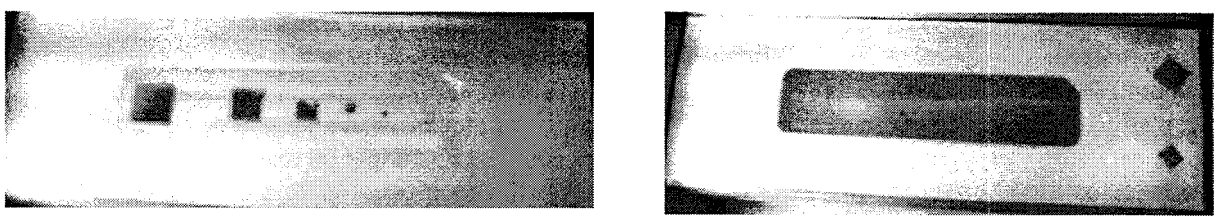

(a) (b)

Figure 17. Layup of Grafoil, (a) beneath U-Mo foil and (b) in Al-Al interface.

Tantalum is a refractory metal (melting point ~3000°C) that can be procured as a thin foil. The 0.0005-in. foil was cut into small strips and folded over on itself to form squares (sizes used measured nominally, on the square 1 cm, 0.5 cm, 0.25 cm and 0.125 cm). The double thickness was introduced to provide an interface that was less likely to bond (Ta to Ta) than the tantalum to Al. Five pieces of the tantalum foil were introduced underneath the U-Mo foil and a single (not pictured) square was placed at the edge of the plate (Figure 18).

c. PRODUCT DISCLAIMER—References herein to any specific commercial product, process, or service by trade name, trademark, manufacturer, or otherwise, do not necessarily constitute or imply its endorsement, recommendation, or favoring by the U.S. Government, any agency thereof, or any company affiliated with Idaho National Laboratory.

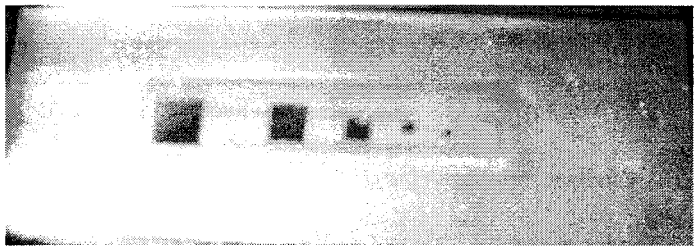

Figure 18. Layup of Ta foil (all are double thickness).

Yttrium oxide (Y_2O_3 or yttria) is used as a refractory coating both for its high temperature stability and its chemical stability. The yttria used "Type Y" aerosol that is composed of yttria, several volatile components and a small amount of binder. The material was applied to the Al cover plate by masking the plate with blue painter's masking tape and cutting out several holes (nominally sized, on the square 1 cm, 0.75 cm, 0.5 cm, 0.25 cm and 0.125 cm). The yttria was then spray painted on in three light coats (total thickness unknown) and allowed to dry prior to moving the tape mask. Examination of the yttria under slight magnification showed a porous layer. The yttria regions were applied in three rows: one to be over the foil, one to be in the clad to clad region, and another along the edge of the plate (Figure 19).

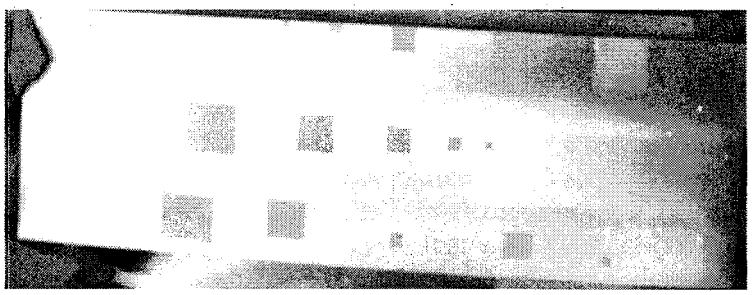

Figure 19. Yttria applied to cover plate.

Aluminum oxide is readily formed on the surface of Al and is inherently stable, but it typically has a thickness measured in nanometers. Anodizing, a process where a much thicker and more stable oxide is forced onto the plate through specialized electroetching was used to place a barrier of oxide onto the cover plate. The anodizing was performed in sulfuric acid under an electrical potential of 30 volts DC. The ideal process temperature of 0–5°C was not achieved (only ~15°C could be reached). The process was conducted for 60 minutes. After anodizing the plate was further processed for 5 minutes in boiling water (known as "sealing" the oxide coat, which forms as a porous cellular layer). The thickness (and quality) of the applied anodized coat were unknown. As the entire plate was anodized the plate was selectively cleaned using a rotating brush. Areas of oxide were left measuring (nominally) on the square 1 cm, 0.75 cm, 0.5 cm, 0.25 cm, and 0.125 cm. The back side of the plate was left uncleaned. Like the yttria plate, the anodized regions were done in three rows: over the foil, in the clad to clad region, and on the edge of the plate (Figure 20).

Figure 20. Oxide regions on cover plate.

A polymeric film was used to produce a debond both by interrupting the bonding between the layers and by producing gas during the HIP process. Polyimide was chosen because it is commonly found in thin film form and because of its thermal stability (ideally to have the contaminant survive the initial bakeout (315°C), but be decomposed during subsequent processing). DuPont™ Kapton® 50HN film was used. This material is 0.0005 in. thick and is stable to ~400°C. The material was cut into small squares. The total material used for this plate was kept low in an attempt to avoid cross contamination of the other plates in the HIP run. The materials used measured, nominally, on the square 0.25 cm and 0.125 cm. The film was placed to be underneath the U-Mo foil, in the cladding to cladding interface and at the edge of the bonded plate (Figure 21).

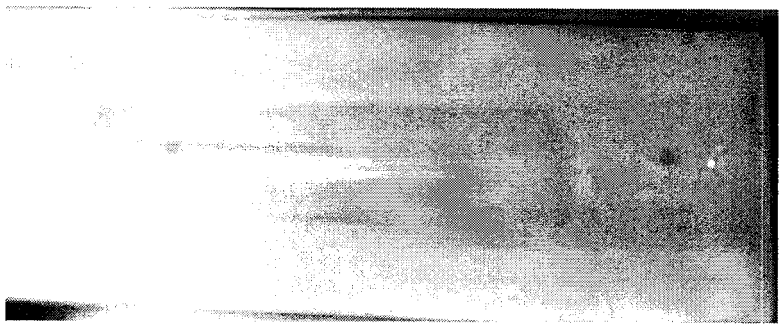

Figure 21. Polyimide film on Al plate.

3.1.1.4 HIP Process

The HIP run proceeded in the standard fashion for the production of mini-plates. The assembled plates were welded inside a stainless steel can, helium leak checked, evacuated at 315°C for 3 hours prior to closure welding. The completed can was placed in the HIP and processed at 560°C for 90 minutes (not counting temperature ramp up and down) and a pressure of ~100 MPa. Following the cool down the can was removed from the HIP and cut open. The plates were stamped and surface sanded (to allow a cleaner UT transmission and achieve an acceptable surface finish).

3.1.1.5 Analysis

The as-HIPed plates were analyzed in the UT scanner using the standard process for mini-plates, then the mini-plates were blister annealed at 485°C for 30 minutes. To prevent severe warping during the annealing, the plates were placed in constraint fixtures—two steel plates on either face of the Al fuel plate bolted together. After cooling to room temperature, blisters were noted and indicated with a marker (raised areas are difficult to photograph) and the plates were again examined in the UT scanner. Despite the constraint fixture, noticeable warping was readily visible in every plate after the blister anneal.

3.1.1.6 Results

The control plate (63-6) showed no debond indications during the first UT analysis, no blisters were noted after the blister anneal, and only a minute indication of a debond in a region near the foil (Figure 22).

3.1.1.7 Yttria Layer Defects

The yttria layer defects were designed to simulate porous layers applied to the final/clad interface prior to HIPing. It was postulated that these layers may include disposal gases that may coalesce during heat treatment.

The yttria-coated plate (63-5) showed no debonds in the as-HIPed condition, though the regions where the Y_2O_3 was applied were apparent as darker than the baseline transmission. Only two blisters were noted after blister annealing, which corresponded with the two largest regions in the clad-to-clad region. The final UT showed that the transmission had markedly degraded in the clad-to-clad region, had slightly degraded in the foil region, and had improved slightly along the edge (partially obscured in both scans by the fixturing) (Figure 23).

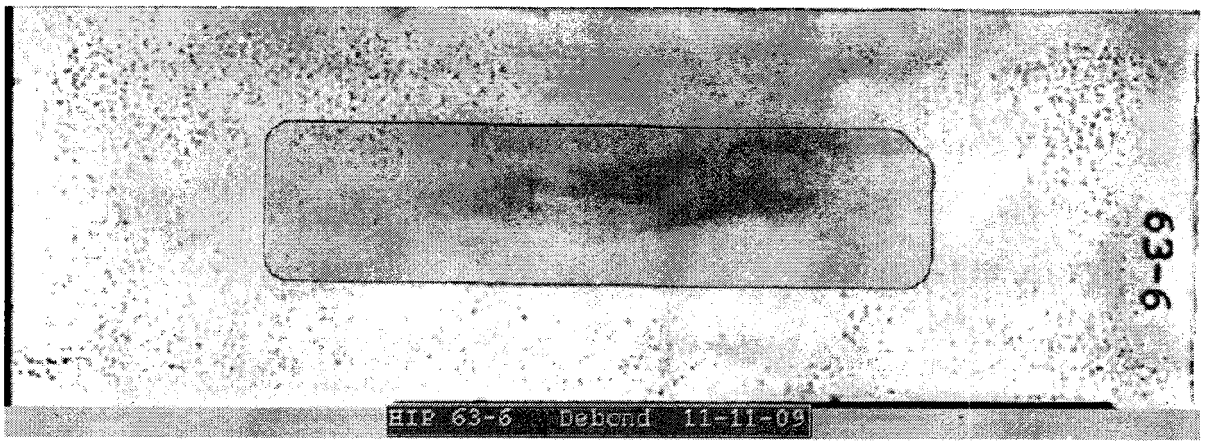

(a)

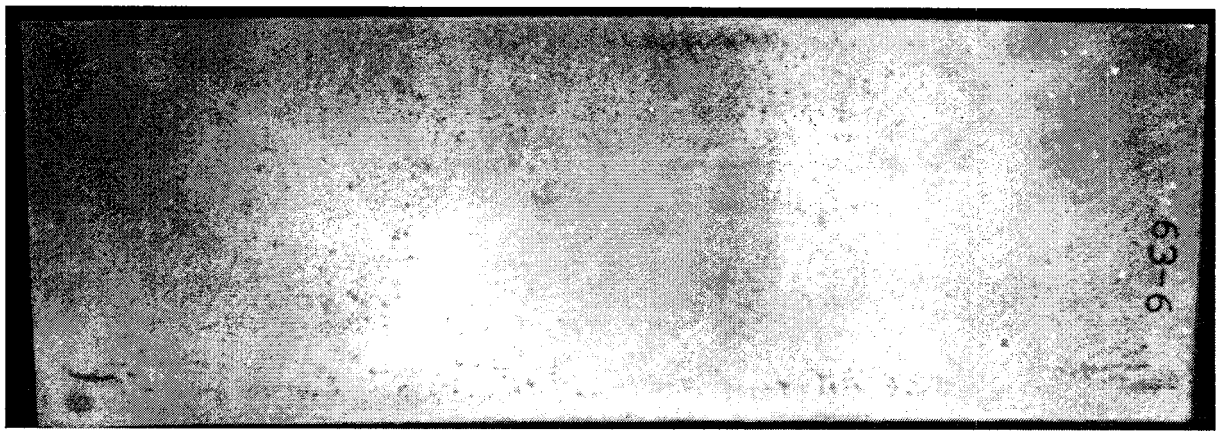

(b)

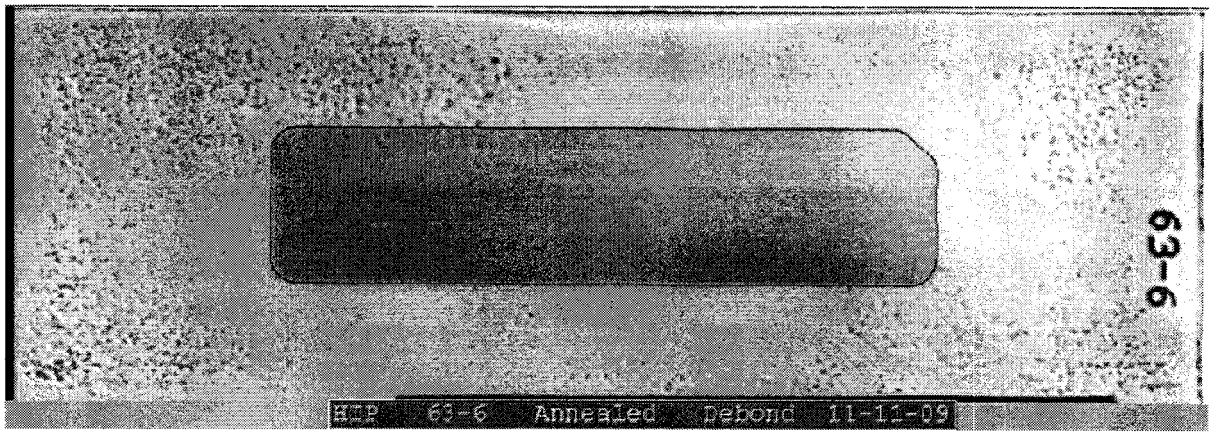

(c)

Figure 22. Control plate. (a) as-HIPed, (b) blister annealed (no blisters noted), (c) UT scan of annealed plate.

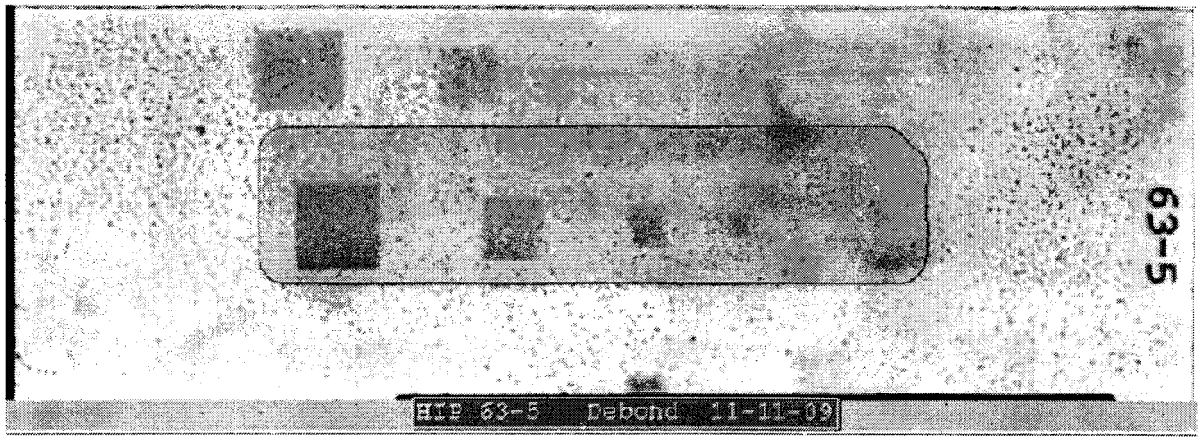

(a)

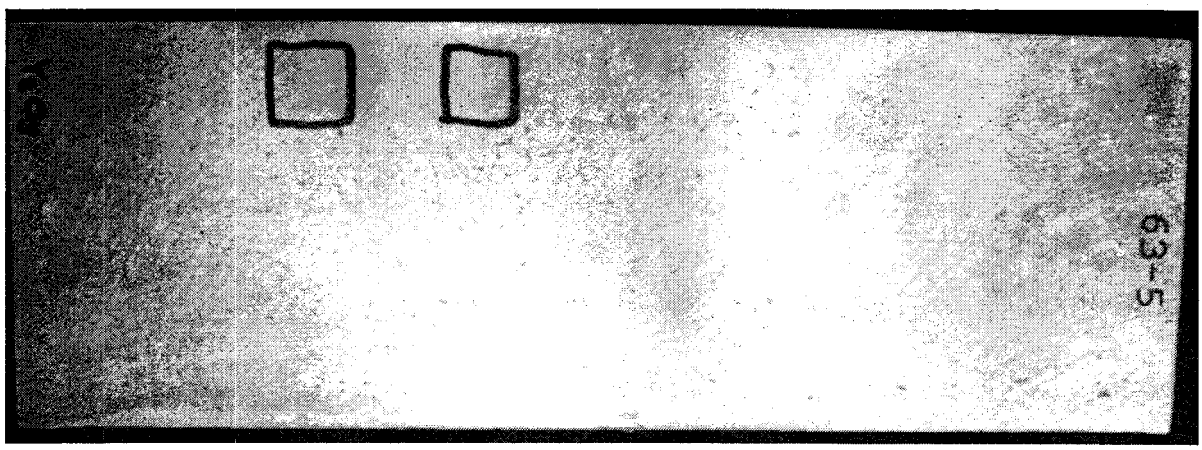

(b)

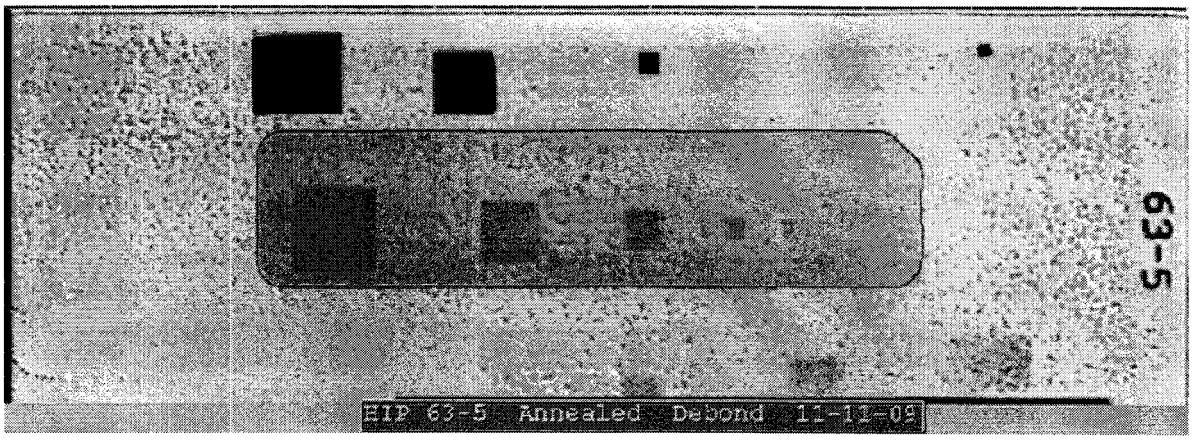

(c)

Figure 23. Yttria coated plate. (a) as-HIPed, (b) blister annealed (two blisters noted), (c) UT scan of annealed plate.

3.1.1.8 Anodized Surface Defect

The anodized defect plates were designed to simulate areas of incomplete surface cleaning. These plates (63-4) showed no indication of debonds in any of the examinations (Figure 24). This indicates that those types of defects have a limited affect on as-fabricated bond strength.

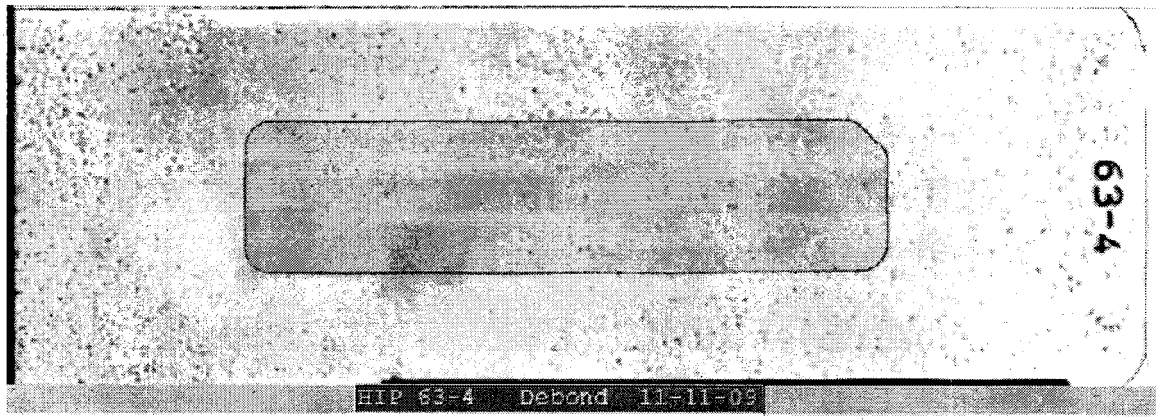

(a)

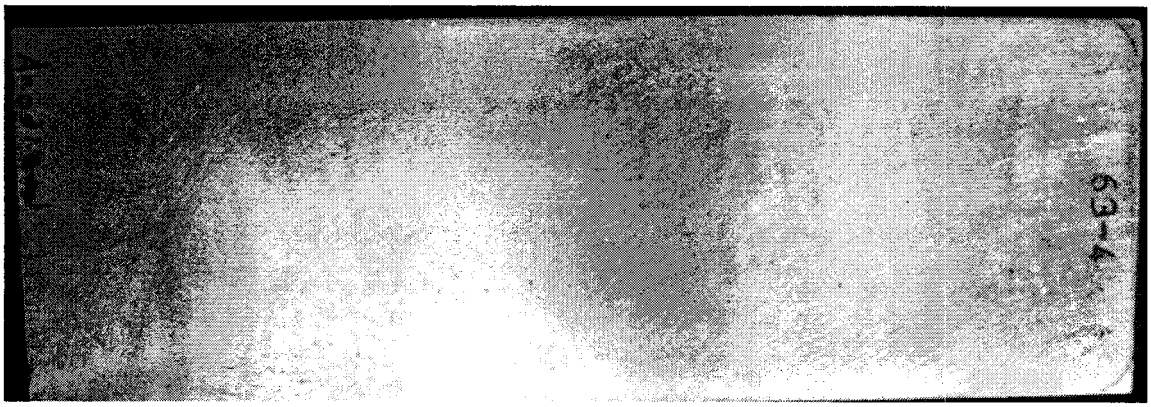

(b)

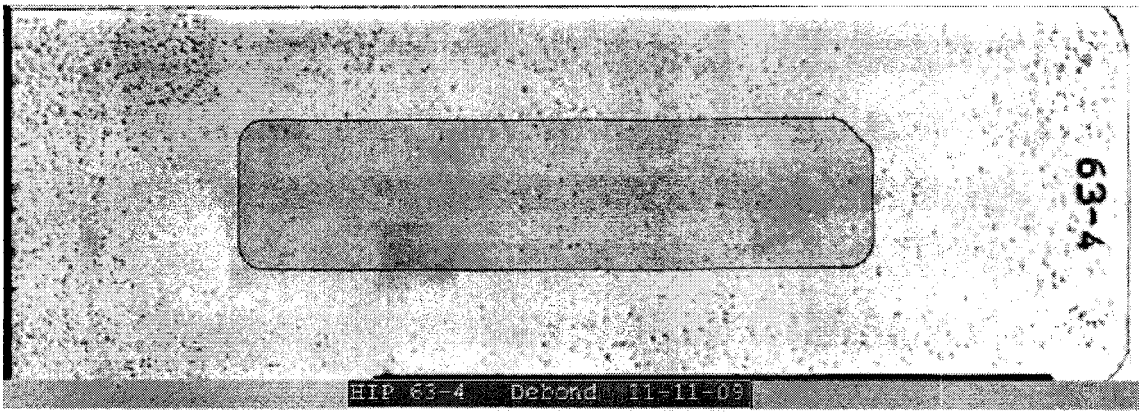

(c)

Figure 24. Anodized plate. (a) as-HIPed, (b) blister annealed (no blisters noted), (c) UT scan of annealed plate.

3.1.1.9 *Tantalum Foil Defects*

The plate containing the tantalum foil (63-3) showed only one region of debond in the as-HIPed condition although the faint outline of the foils can be found in this scan (particularly in the foil region). The debond region lies at the edge of the plate underneath the stamp. The blister annealing revealed no raised blisters. The post blister annealing UT scan showed additional debond regions at the edges of the tantalum foil that were likely caused by differences in thermal expansion between the U-Mo, Ta, and Al (Figure 25).

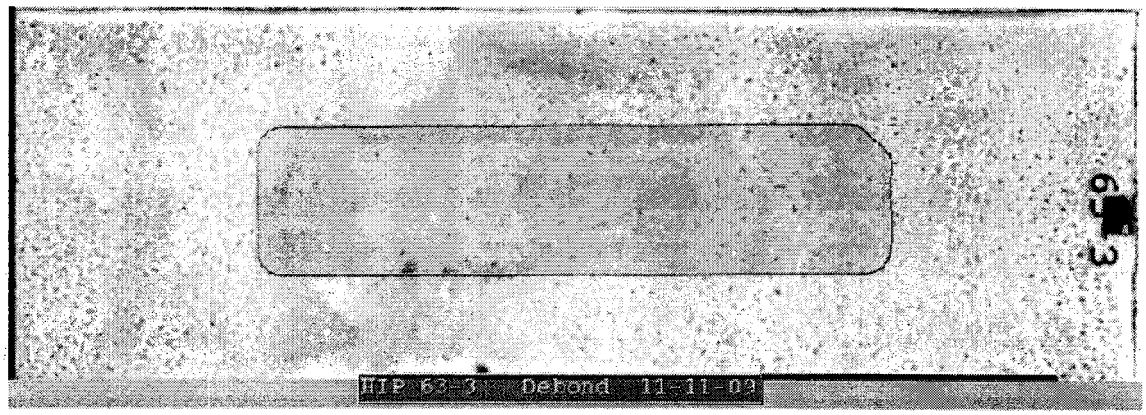

(a)

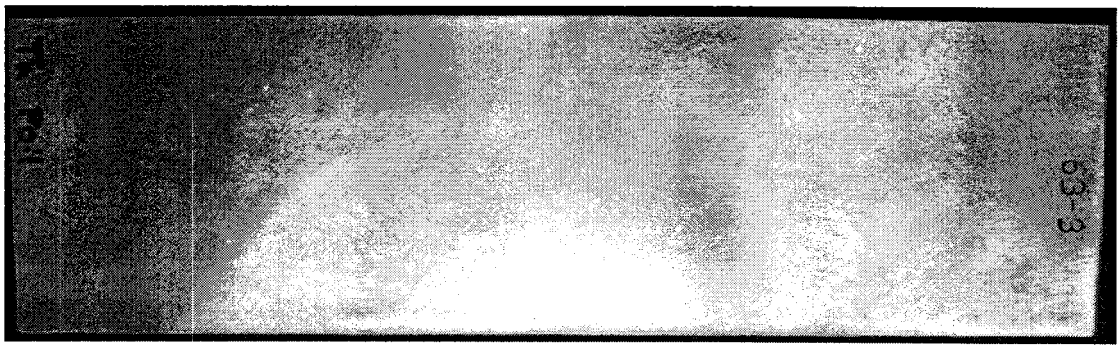

(b)

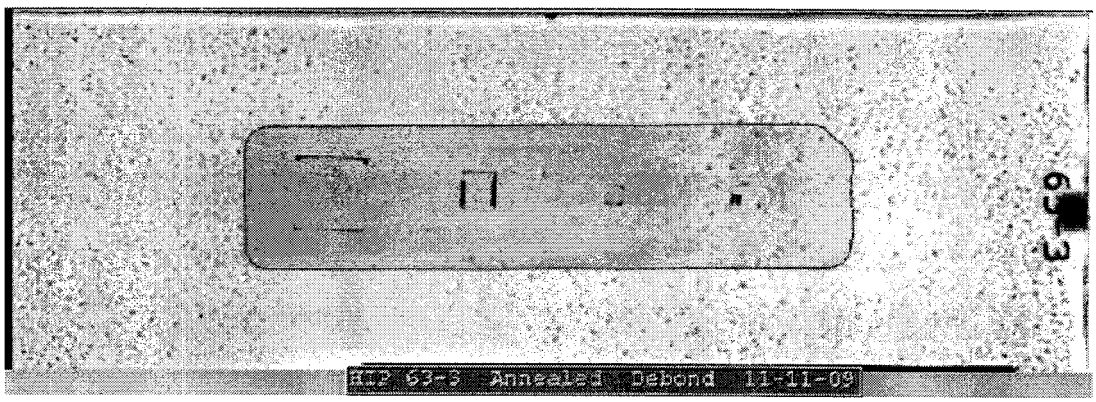

(c)

Figure 25. Tantalum foil plate. (a) as-HIPed, (b) blister annealed (no blisters noted), (c) UT scan of annealed plate

3.1.1.10 Grafoil Defects

The Grafoil defects were designed to simulate areas contaminated with stray material during the fabrication process.

The Grafoil plate showed debonds over all the regions where the foil had been placed (the smallest foil region [0.005 in.] can barely be seen). The blister annealed plate showed blisters over all, except the smaller foil regions. It is noted that the blisters only appear on the side nearest the cladding surface—the region under the U-Mo foil is nearer to the unstamped face of the plate. The UT scan of the blister annealed plate reveals no new debond regions, but the existing debonds have somewhat clarified (Figure 26).

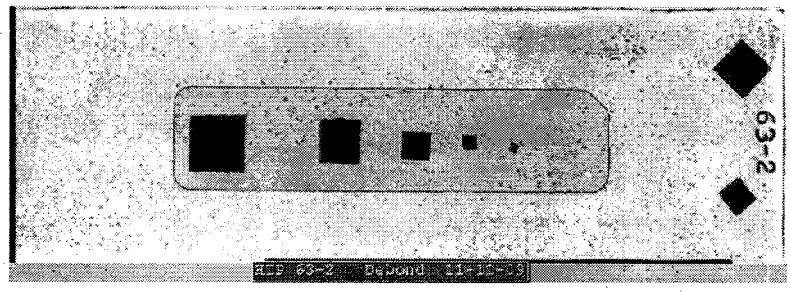

(a)

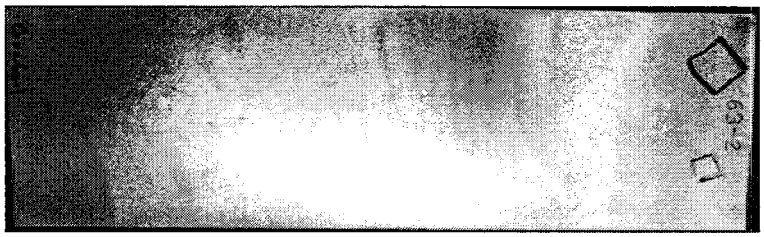

(b)

(c)

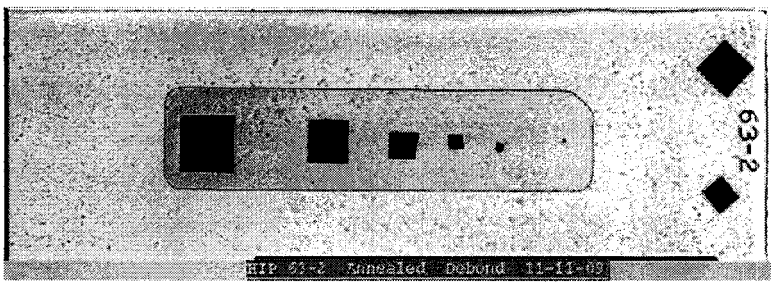

(d)

Figure 26. Grafoil foil plate. (a) as-HIPed, (b) blister annealed (blisters marked), (c) blister annealed (obverse—blisters noted), (d) UT scan of annealed plate.

3.1.1.11 Polyimide Film Defect

The polyimide film defect was designed to simulate a defect caused by gas entrapped in the fuel plate. The polyimide film plate (63-1) showed clear debonds over all five locations were the film was placed. The blister anneal showed clearly defined blisters over all, except the region at the edge of the plate. Unlike the other plates, some blisters (in the clad-to-clad region) were visible on both faces of the plates. The post blister annealed UT scan is virtually identical to the as-HIPed scan (Figure 27).

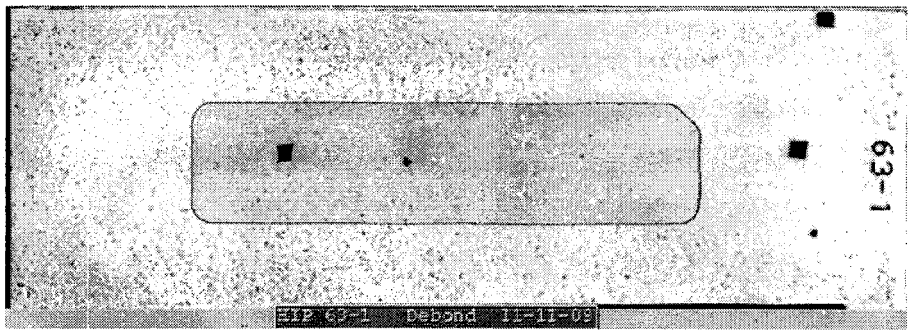

(a)

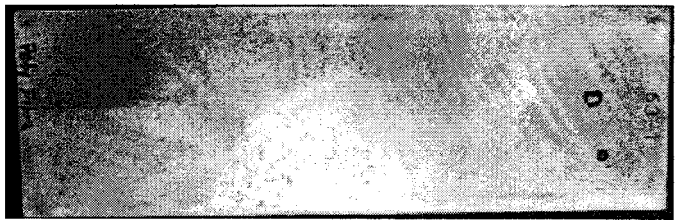

(b)

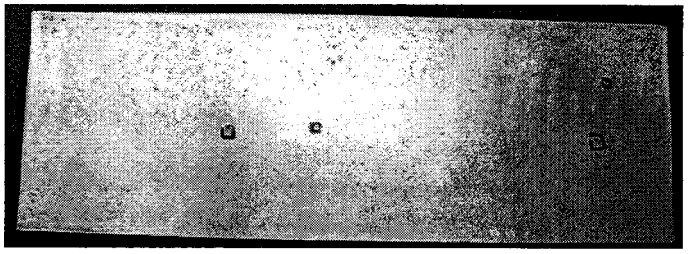

(c)

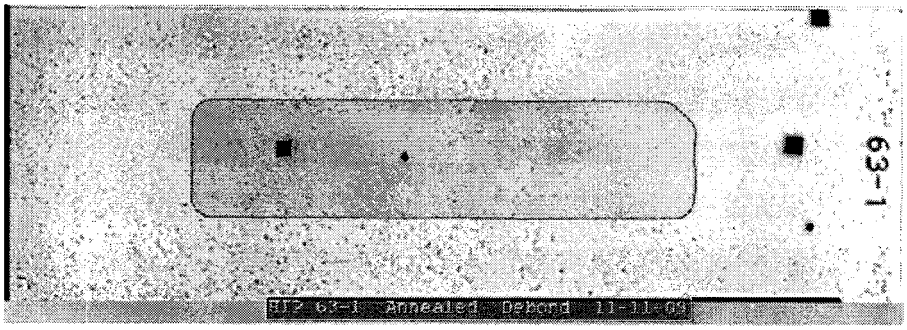

(d)

Figure 27. Polyimide film plate. (a) as-HIPed, (b) blister annealed (blisters marked), (c) blister annealed (obverse—blisters noted), and (d) UT scan of annealed plate.

3.1.1.12 Discussion

In every case in this HIP experiment the blisters that were manifested by the blister annealing were shown previously in the as-HIPed UT scan of the plate. There were, however, several instances where debonds were noted in the as-HIPed UT scan, but blisters failed to materialize in several locations where debonds were noted in the as-HIPed scans (Table 4).

Table 4. Comparison of debond test results.

Method	First UT	Blisters	Second UT
Control	No debonds or indications[d]	No blisters	Small debond no indications
Y_2O_3	Several indications, no debonds	2 blisters on largest of clad-to-clad bonding	4 debonds in clad-to-clad region, "indications" in other regions
Anodized	No debonds or indications	No blisters	No debonds or indications
Ta Foil	Debond on edge foil, faint indication on other foils	No blisters	Debond on edge foil, thin debonds on some edges of other foils
Grafoil	Debonds on all foils locations	Blisters on all but smaller foils	Debonds on all foil locations
Polyimide	Debonds on all film locations	Blisters on all but the film located at the plate edge	Debonds on all film locations

In general, blisters were only formed over regions with larger debonds. The exception was the polyimide film where all the film locations (except where the film was located on the edge of the plate—see below) formed clearly defined blisters. The polyimide film was the only method to produce blisters that were noted on both sides of the plate. Since all of the interfaces in the plate are closer to one of the surfaces, the blisters tend to deform the material where the overlaying material is thinner—and inherently weaker. The only blisters in the polyimide plate that appeared on a single side were placed beneath the U-Mo foil where the added rigidity of the fuel material is judged to have constrained the blisters to a single side.

No blisters were formed along an edge of one of the plates. There were strong debond indications at the edges of the plates in both the tantalum and the polyimide plates. Assuming that the blisters are remnants of gas pocket expansion (either by gas generation or by thermal expansion) the expanding gas must be fully contained in order to exert the pressure to deform the surface of the plate and form a blister. In the regions where a suitable contaminant or gas pocket intersects a free surface, the expanding gas escapes from the plate without forming a blister (although still leaving a debonded area that is readily visible with a UT scan.

The yttria plate is of some note as there were some interesting changes resulting from the blister annealing step. Prior to the blister anneal the UT scan only showed "indications," but nothing that would be interpreted as a debond. The blister anneal test yielded only two blisters over the larger of the two regions in the clad-to-clad region. These two blisters showed clear debonds in the UT scan, but other debonds were found in this UT scan that did not appear as blisters on the plate surface. The other two regions where defects were introduced (the fuel foil and along the edge) did not form blisters and did not show as debonds in either the blister anneal test or the subsequent UT scan. In either case, any entrapped

d. A "debond" is any area that appears black on the UT scan, and "indication" is an area that appears as grey. For reference, the fuel phase (either dispersion or monolithic) appears as an indication due to sound wave attenuation through the higher density interfaces.

gas would have an escape avenue. The regions along the edge would have a clear path out of the plate while the region over the foil were in contact with the Zr layer, which is a good "getter" and may have tied up any evolved gases.

3.1.1.13 Summary of Engineered Defect Studies

Blisters formed only in locations where there were existing indications that were identifiable in the UT scan of the as-HIPed plates.

Not all indications resulted in blisters (especially in smaller debond regions), demonstrating that there is some debond threshold below where a blister will not form, yet it still shows debond indications visible to UT. This suggests that high resolution UT scanning is a conservative substitute for the blister anneal treatment and subsequent visual exam for blisters.

It was also evident that blisters will not form unless there is gas trapped inside the plate. The gas may come from either residual voids remaining from the assembly process or from outgassing of an included contaminant. All of the blisters can be traced back to materials that either decomposed during the thermal history of the plate or had probable porosity. Gas pockets that are externally vented (see the debond located at the edge of the polyimide plate in Figure 27) will not form blisters. This suggests that fuel designs requiring consolidation of powders during fabrication be subjected to a blister anneal prior to UT scanning to ensure that diffuse gases coalesce into a recognizable indication.

It was also observed that the blister annealing introduces warping in monolithic fuel plates. Therefore, the blister annealing thermal treatment can introduce degradation into a fuel plate that may take it from an acceptable to an unacceptable condition. Based on these observations it is recommended that UT scanning be used to characterize bonding as the reference process monolithic fuel plate design.

3.1.2 RERTR-12 Blister Anneal Summary

Prior to RERTR-12, blister annealing has not been routinely performed on monolithic U-Mo fuel plates. Therefore, the blister annealing results presented here provide new insight into the potential advantages and disadvantages of performing blister annealing on this type of fuel as part of the fabrication/inspection process.

The RERTR-12 test involves 56 fuel mini-plates, all produced by HIP Al-6061 alloy cladding of Zr co-rolled U-10Mo fuel foils. The first insertion will involve four capsules and 32 mini-plates. Fabrication is in progress. Blister annealing was carried out on all of the RERTR-12 mini-plates after the plates had been machined to final thickness and undergone an initial UT debond scan.

The first set of mini-plates were blister annealed unconstrained and exhibited no-blisters; however, the originally flat plates became severely warped, with significant two-dimensional out-of-plane bending observed (e.g., >0.5 in. of bending was observed across the ~5 in. length of the as-HIPed fuel plate). Such deformation results from a combination of redistribution of residual stresses contained within the fuel foils and the thermal expansion mismatch between the cladding and the fuel, which are unique to the monolithic fuel (i.e., this is significantly different from the situation in the case of dispersion fuels). In any case, such dimensional instability makes the subsequent final plate fabrication steps extremely difficult and is therefore highly undesirable.

Blister annealing on subsequent plates was performed using custom-designed retaining fixtures to constrain the plates in effort to keep them flat; however, significant plate warping and dimensional instability was still observed, albeit less severe than in the case of unconstrained blister annealing.

Of the blister annealed plates in this study, three plates produced visible blisters and were rejected. These particular plates each showed pre-existing debonded regions in the as-HIPed condition, identified clearly by the ultrasonic testing (UT) scan. The defects observed in these particular fuel plates result from the fuel foil not remaining properly aligned within the machined pocket of the Al cladding during HIP, leaving behind remnant voids that do not fully collapse during HIP. This type of defect has been observed occasionally in the UT scans of HIP plates, and is a cause for rejecting the plates based upon UT. It is important to note that no blisters have been observed in fuel plates that did not contain pre-existing debonds readily identified in the initial UT scan.

In a few cases, the post-blister annealing UT scans on plates that did not contain any visible blisters (and would therefore pass the blister anneal test) reveal that it is likely that some degradation was introduced into the otherwise acceptable fuel plates during blister annealing, as evidenced by the appearance of small debonds or debond indications that were not previously observed in the initial UT scan. Therefore, not only can blister annealing degrade acceptable fuel plates, but the blister inspection itself would not necessarily reveal the presence of any such damage introduced.

In summary, it is apparent that UT scanning is a more sensitive, acceptable method of detecting the presence of defects in HIPed monolithic fuel plates, including identification of the types of defects that can give rise to visible blisters in the blister annealing test. Blister annealing results in severe warping and dimensional instability in fuel plates that significantly complicates subsequent fabrication steps. In addition, blister annealing may introduce degradation into otherwise acceptable fuel plates, while not detecting the presence of certain resulting defects so introduced. For these reasons, in the case of HIPed monolithic fuel plates, blister annealing does not add value to the fuel plate fabrication and inspection process.

3.2 Delaminations Due to Fuel Performance

The second pathway that can lead to a delaminated fuel plate is through breakdowns in fuel performance. Identification of the fuel system characteristics that may lead to these types of behavior is often the primary purpose of the fuel testing. An irradiation-induced delamination is possible when the fuel/clad interface is subjected to mechanical stress due to thermal stresses or fuel meat swelling, for example. While the effort described in the previous sections is applied to demonstrate that the as-fabricated fuel/clad bond strength is adequate, in some fuel designs the fuel/clad bond strength may degrade during irradiation due to fission product migration and other metallurgical processes. When the stresses exceed the bond strength a delamination may develop between the fuel and cladding. Optimization of the as-fabricated fuel/clad bond strength and its irradiation stability is a primary research and development (R&D) focus of the RERTR program. The fuel designs being tested in the RERTR-10 test were specifically oriented toward evaluation of the silicon-modified and Zr barrier interface designs. As was described in an earlier section, the Zr barrier system performed exceptionally well (i.e., no delaminations) and the silicon-modified system exhibited irregular behavior (i.e., some delaminations).

Delaminations have been observed in fuel plate tests other than L1P145 without providing any indication of abnormal surface oxidation behavior. Two Si-modified interface fuel plates and one Zr barrier fuel plate are shown in Figure 28. The two Si-modified plates behaved very similarly during irradiation in that both plates had significant areas of delamination (Figure 29). Both fuel plates were fabricated using the same process and were subjected to similar irradiation conditions. The post irradiation neutron radiographs taken of the fuel plates show the presence of internal cracks in the fuel foil in the regions underneath the delaminations. It is not clear if the cracks formed before or after the delamination. It is clear from the photographs of the fuel plates that minor surface oxidation variations occur over the delaminated sections due to temperature variations that occur due to delamination. However, the RERTR-10A L1P145 fuel plate blister did not form over one of these areas or seem to have any correlation with the delaminated areas (Figure 30).

From this examination it is concluded that while delamination may be a contributing factor to the formation of abnormal oxidation behavior (by increasing the local surface temperature), it does not act as an initiator for the formation of blister defects like that observed in the RERTR-10A fuel plate.

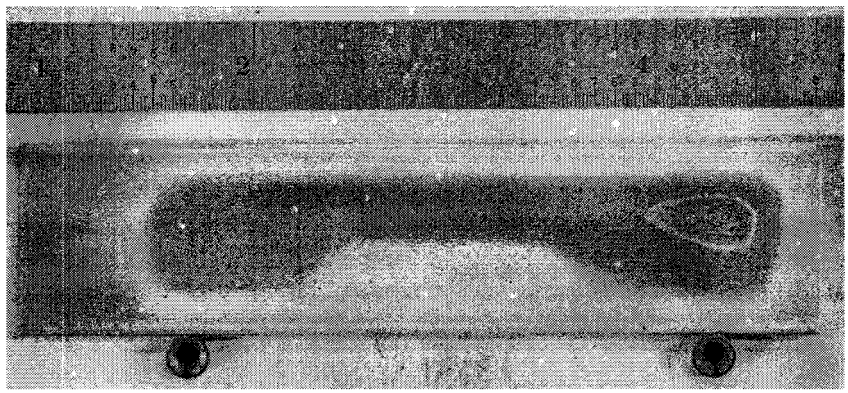

(a)

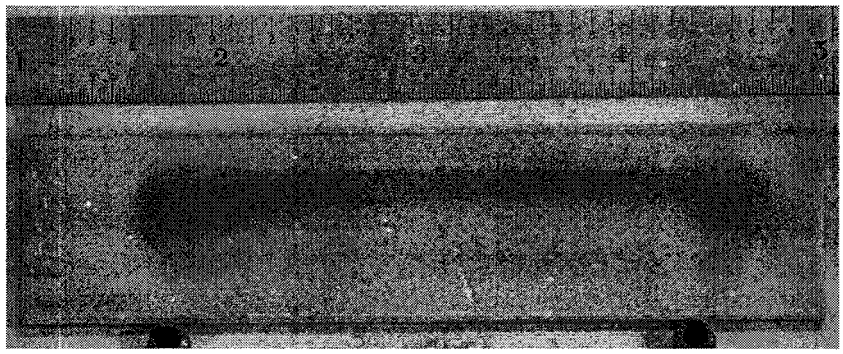

(b)

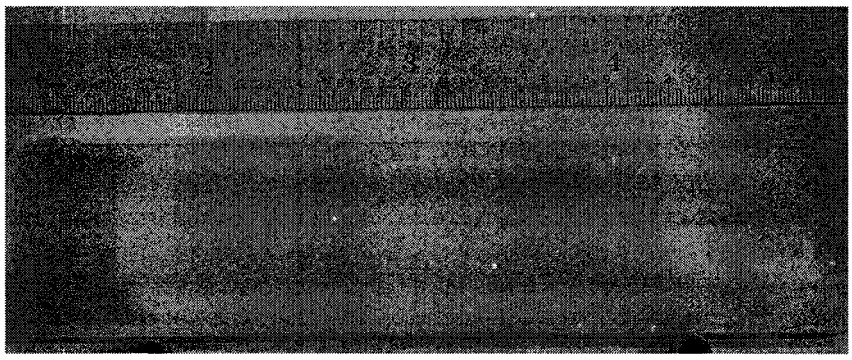

(c)

Figure 28. Photographs of the several fuel plates from the RERTR-10A test. (a) L1P145 – silicon-modified (note discoloration on lower edge of plate over the delamination, note blister at bottom of plate), (b) L1P202 – silicon-modified (note discoloration on lower edge of plate over the delamination), and (c) L1P12Z – Zr barrier.

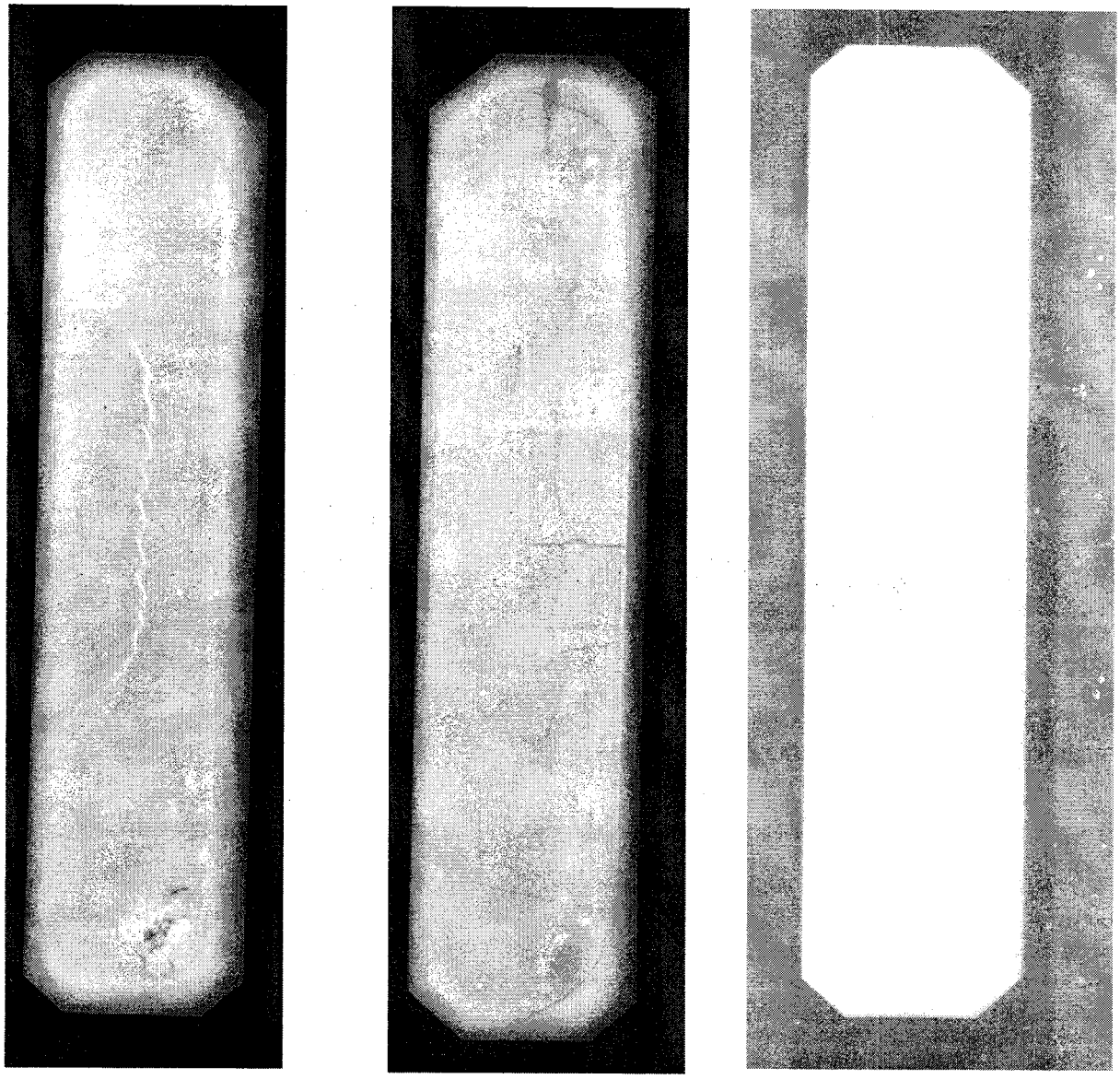

Figure 29. Neutron radiographs of the three fuel plates shown in Figure 28. Note that for the silicon-modified plates, the internal cracks in the foil coincide with the delaminations and surface discoloration observed on the surface. It is also significant that cracking is not observed in the Zr barrier fuel plate.

Figure 30. Metallographic cross sections taken from the mid-plane of the three fuel plates shown in Figure 28. The images show a significant difference in the extent of cracking that occurred in the silicon modified plates compared to the Zr barrier plate.

3.3 Mitigations for Fuel/Clad Bond Defects

The studies conducted to evaluate debond identification and formation show that the presence of a pre-irradiation debond defect was very unlikely. However, to further limit the potential for the formation of an abnormally oxidized area in a fuel plate, several mitigations for as-fabricated debonds have been proposed. These mitigations are aimed at reducing the potential that a fuel plate with an as-fabricated fuel/clad defect is inserted into ATR.

The specifications used to screen the fuel/clad interface for regions of debond using UT scanning (rather than the blister anneal) will be enhanced by including accept/reject criteria for acceptance. The size of allowable as-fabricated defect will be established for each test based on the specific thermal hydraulic conditions of that test.

The blister anneal test has been applied to the RERTR-12 test while the UT scan based on allowable debond criteria is more completely developed. Because the RERTR-12 test uses mini-plates, blister anneal could be performed. The UT scan criteria will be concurrently refined so that it screens for debonds that may result in a blister, and does not unnecessarily reject parts with non-detrimental/minor debonds.

The blister anneal test will continue to be used for screening of all dispersion fuel plates.

4. SUMMARY

The RERTR-10A test was conducted to evaluate the performance of a modified fuel/clad interface design under irradiation. The test clearly showed the excellent performance of the Zr diffusion barrier based design and the marginal performance of the silicon design at very severe conditions. As a result, the silicon design will be dropped and the future testing will focus on the Zr design.

Formation of a blister on the surface of one plate during this test was observed. Root cause analysis suggests that the blister was caused by excessive local surface corrosion that occurred due to inadequate formation of a protective boehmite layer.

The fuel plate sensitivity may have been enhanced by the presence of fuel/clad delamination near the defect. An evaluation conducted to identify if an as-fabricated defect may have been a contributing factor to the breach. The studies showed that the UT scan process is more conservative than the blister anneal and should be applied formally in the fuel specifications.